Review

Review on Channel Estimation of Reconfigurable Intelligent Surface Assisted Wireless Communication System

Yun Yu [1],[‡] (ID), **Jinhao Wang** [1],[‡] (ID), **Xiao Zhou** [1],[3],[*] (ID), **Chengyou Wang** [1],[3] (ID), **Zhiquan Bai** [2] (ID) **and Zhun Ye** [1]

1   School of Mechanical, Electrical and Information Engineering, Shandong University, Weihai 264209, China
2   School of information Science and Engineering, Shandong University, Qingdao 266237, China
3   Shandong University–Weihai Research Institute of Industry Technology, Weihai 264209, China
*   Correspondence: zhouxiao@sdu.edu.cn; Tel.: +86-631-568-8338
‡   These authors contributed equally to this work.

Abstract: With the dramatic increase in the number of mobile users and wireless devices accessing the network, the performance of the fifth generation (5G) wireless communication systems has been severely challenged. Reconfigurable intelligent surfaces (RIS), one of the potential technologies for the sixth generation (6G), has received a lot of attention. Since it is easier to deploy, consumes less power, and is inexpensive. RIS is an electromagnetic metamaterial that serves to reconfigure the wireless environment by adjusting the phase, amplitude and frequency of the wireless signal. To maximize channel transmission efficiency and improve the reliability of communication systems, the acquisition of channel state information (CSI) is essential. Therefore, an effective channel estimation method guarantees the achievement of excellent RIS performance. This paper conducts a comprehensive investigation of the existing channel estimation methods of RIS, analysis and comparison of channel model building and CSI acquisition schemes in different frequency bands, in addition to a comprehensive description of generic channel estimation methods, with a focus on the application of deep learning. Finally, we conclude the paper and provide an outlook in the future development of RIS channel estimation.

Keywords: wireless communication system; sixth generation (6G); reconfigurable intelligent surface (RIS); channel estimation

---

1. Introduction

With the explosion of mobile data and the demand for better quality services, effective and reliable communications are becoming important increasingly. The advent of the Internet of things (IoT) marks the interconnection of everything, while providing great convenience. It is a great challenge for information transmission. In the past few decades, researchers have worked to improve the quality of service of wireless channels. Now, it is important to find a technology with low energy consumption while ensuring the quality of service. In the fifth generation (5G), it may face problems such as enable to meet larger connection capacity and more energy loss. To solve these problems, the development of the sixth generation (6G) has become a hot topic of increasing interest [1].

The development of 5G has become saturated increasingly, and in the upcoming era of IoT, communication systems need greater spectral efficiency and higher communication effectiveness. Massive multiple input multiple output (MIMO) technology has become to be the core technology of 5G, in which a large number of radio frequency (RF) antennas lead to high hardware costs and maintenance costs. The short propagation distance of electromagnetic waves in the high frequency bands and the limited coverage of electromagnetic waves require an increase in the number of base station (BS), which will further increases the hardware and maintenance costs of 5G. At the same time, the dense distribution of BS and antennas reinforces the signal interference of 5G, deteriorates the performance of the network, increases the computational complexity of network coordination, and

faces a serious dilemma in the development of 5G. We need an effective solution to realize the future of 6G [2,3].

To meet the requirements of more superior performance and sustainability of 6G, many options have been proposed. Reconfigurable intelligent surface (RIS) has received much attention from academia and industry as a potential technology for 6G. RIS, also called intelligent reflecting surface (IRS). RIS is a new paradigm of electromagnetic metamaterials, which is composed of many of passive reflective elements. It can reconfigure the wireless communication environment by intelligently modulating electromagnetic waves through digital coding to modulate the amplitude, phase and frequency of the signal, which can improve the performance of wireless communication systems [4,5]. In 5G, millimeter wave (mmWave) as one of the main methods can increase the communication capacity to solve the spectrum shortage problem significantly. However, its small wavelength drawback can lead to transmission difficulties [6].

The coverage capacity of the signal can be increased by arranging RIS. Prior to the proposal of RIS greatly, techniques such as active frequency selective surfaces have been proposed [7], followed by theories such as space-time modulated digital coding metasurfaces, which laid the foundation for the emergence of RIS [8]. Furthermore RIS can increase the network capacity by changing the phase shift to complete passive beam assignment [9]. RIS has been developed continuously and nowadays there are not only reflective RIS but also transmissive RIS with the advantages of higher aperture efficiency and operating bandwidth [10]. More than that, RIS has the advantages of low power consumption and low cost compared to amplify and forward relay system due to its passive characteristics [11]. The above advantages of RIS make it useful in high frequency bands, orthogonal frequency division multiplexing (OFDM) [12], non-orthogonal multiple access (NOMA) [13], and multi-antenna systems. However, to perform the role of RIS and accomplish effective and reliable wireless communication, it is required to obtain accurate channel state information (CSI) using channel estimation techniques, which is a great challenge. There have been many studies in channel estimation, and this paper provides a basic overview of RIS channel estimation.

We first analyse the full range of transmitted frequency wireless signals briefly, and then focus on the 6G band. Channel estimation plays a critical role in the performance of wireless communication systems, this paper overviews RIS channel estimation schemes in various scenarios. In Section 2, we published reviews about RIS channel estimation, which are based on the main directions and main contributions. In Section 3, channel estimation schemes in different frequency bands are introduced. In Section 4, different channel estimation signal processing algorithms are introduced, and this paper is concluded in Section 5.

Notations: The scalar, vector, and matrix are lowercase, bold lowercase, and bold uppercase, i.e., a, $\boldsymbol{a}$, and $\boldsymbol{A}$, respectively. $(\cdot)^{\mathrm{H}}$ denotes conjugate. $\boldsymbol{I}_M$ denotes the $M \times M$ identity matrix. $\mathcal{CN}(\mu, \sigma^2)$ denotes the complex Gaussian distribution with mean μ and variance σ^2. Diag$(\cdot)$ denotes the diagonal matrix whose diagonal entries equal to entries of given vector. $\otimes$ denotes Kronecker product. $\|\cdot\|_{\mathrm{F}}$ denotes Frobenius norm.

2. Objectives and Contributions

Deep learning has developed rapidly in recent years and has been used in many fields due to its advantages in processing complex system data and mining the deep value of data widely. Researchers have studied deep learning-based technologies in RIS-assisted wireless communication systems. Zheng et al. [14] focused on promising research directions and emerging RIS architectures, Pan et al. [15] and Jian et al. [16] outlined channel estimation schemes for RIS assisted communication systems and channel modeling. Table 1 describes the 9 public overviews for RIS assisted wireless communication system, presenting the main direction and major contribution for each overview.

Table 1. Representative overview/survey papers on RIS

Ref.	Year	Main Direction	Major Contribution
Wu et al. [4]	2021	Reflection optimization and channel estimation	Reflection channel models, practical constraint, and hardware architecture
Noh et al. [6]	2022	Channel estimation for RIS-assisted mmWave/sub-terahertz (THz) communication	Technical challenges, channel estimation frameworks, and training signal design
Zheng et al. [14]	2022	Channel estimation and passive beamforming design	Discussed emerging RIS architectures , applications and practical design problems
Pan et al. [15]	2022	Channel estimation, transmission design, and radio localization	Channel estimation, transmission design, radio localization, etc.
Jian et al. [16]	2022	Channel estimation	Wireless communication standards, the current and future standardization activities
Liang et al. [17]	2021	Channel estimation and system design	Reflection principle, channel estimation, system designs, etc.
Chen et al. [18]	2021	Hardware design, channel estimation, etc.	Channel modeling, new material exploration, etc.
Basharat et al. [19]	2022	CSI acquisition, passive beamforming optimization, etc.	Phase-shift optimization and resource allocation
Babiker et al. [20]	2022	Channel estimation	Main recent techniques and various strategies

Specifically, we focus on the RIS-assisted channel estimation models in different frequency bands. A tracing outlook on subsequent signal processing algorithms is given, with the algorithms focusing on techniques related deep learning RIS channel estimation algorithms, such as building end-to-end networks, introducing image processing algorithms and fusing conventional schemes with deep learning. This paper focuses on summarizing the different RIS channel estimation schemes and signal processing algorithms in different frequency bands, considering a comprehensive overview of the existing literature on channel estimation schemes.

3. Channel Estimation in Different Frequency Bands

In the 5G of wireless communications, as the low frequency bands is utilized fully, the target is shifted to the direction of higher frequency bands with higher bandwidth. MmWave technology is considered to be an effective solution to the problem of spectrum resource shortage, and THz with higher spectrum will also become an important direction for future beyond 5G (B5G) and 6G wireless communication systems. Although the communication in high frequency bands can solve the problem of spectrum resource shortage, but due to its small wavelength characteristics, it will produce serious path loss, resulting in small coverage of mmWave, RIS can improve the coverage of its communication at a lower cost. As shown in Figure 1, the mmWave frequency bands is 30 –300 GHz, and its wavelength is only 1–10 mm. The THz has the frequency of 300 GHz–10 THz and it has a much shorter wavelength. The higher frequency band reaches the visible light band, which is 395–750 THz. RIS not only extends wireless coverage, but also plays a role in improving communication quality and expanding communication capacity. However, the optimization of both beamforming and reflection coefficient matrix of RIS transceivers cannot be achieved without accurate CSI, it is crucial to

use efficient, low-overhead and low-complexity channel estimation methods. Due to the difference in frequency bands and hardware architecture, the chosen estimation method will be different. The method chosen will also vary in different system settings such as single input single output (SISO), multiple input single output (MISO), single input multiple output (SIMO) and MIMO. In the following, we outline the advantages and disadvantages of different channel estimation methods in the high and low frequency bands, and discuss representative work and present the basic principles.
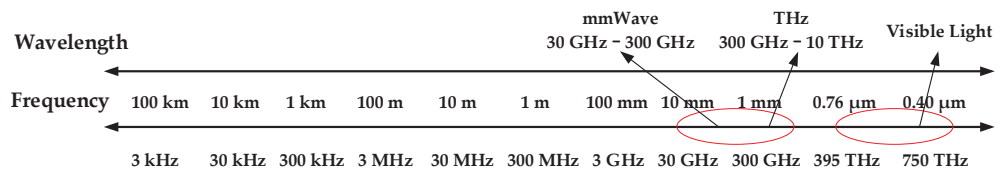

Figure 1. Frequency and bandwidth of wireless radio waves.

In this discussion, since the channel estimation of BS-user equipment (UE) can often be obtained using common channel estimation methods to obtain CSI or directly propagate blocked, only the channel reflected through the RIS is discussed. As shown in Figure 2, we considered an uplink MIMO system model. Assume that the BS is equipped with $M=M_h\times M_v$ antennas uniform planar array (UPA), where M_h is the number of antennas in the horizontal direction and M_v is the number of antennas in the vertical direction. The RIS is equipped with $N=N_h\times N_v$ reflecting elements UPA, where N_h and N_v are the number of reflecting elements in the horizontal and vertical directions, respectively. In this communication system, there are K single antenna users. The channel from the RIS to the BS can be denoted by $H \in \mathbb{C}^{M\times N}$, and the channel from the kth ($k \in K$) user to the RIS can be denoted by $h_k \in \mathbb{C}^{N\times 1}$. The reflection matrix of the RIS element can be denoted by $\boldsymbol{\phi} = [\beta_1 e^{j\alpha_1}, \beta_2 e^{j\alpha_2}, \cdots, \beta_N e^{j\alpha_N}]^T \in \mathbb{C}^{N\times 1}$, where β_n and $\alpha_n (n = 1, 2, \cdots, N)$ denote the reflection amplitude and phase of the nth RIS reflector, respectively [21–23].

As shown in Figure 2, assuming that user k sends the pilot symbol $x_{k,t}$ at time slot $t (t \in T)$, the received signal $y_{k,t}$ at BS can be expressed as:

$$y_{k,t} = h_{d,k}x_{k,t} + H\mathrm{diag}(\boldsymbol{\phi})h_k x_{k,t} + n_{k,t} \tag{1}$$

where n_t represents additive white Gaussian noise (AWGN), assuming $n_t \sim \mathcal{CN}(0, \sigma^2 I_M)$, and σ^2 is noise power. $h_{d,k}$ is the direct channel between the BS and user k. Since this paper assumes that the direct channel is blocked, therefore $h_{d,k} = 0$. The cascade channel G can be expressed as:
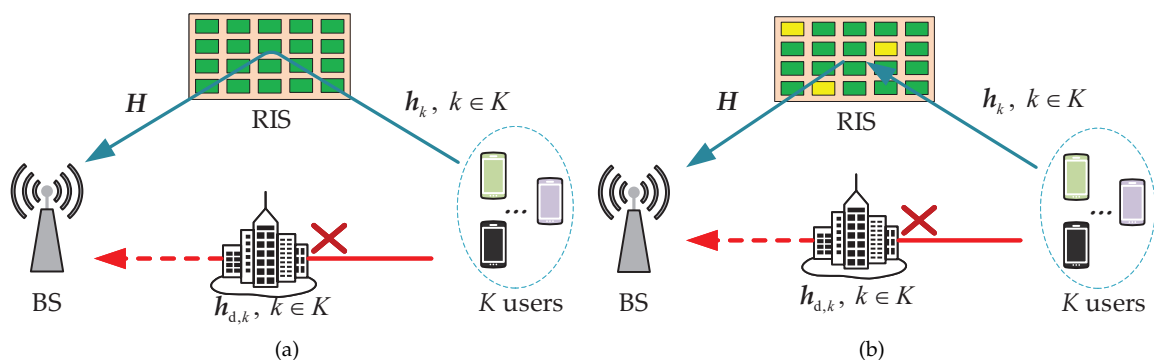
$$G = H\mathrm{diag}(h_k) \tag{2}$$

Figure 2. A RIS aided multi-user MIMO system consisting of a BS with M antennas, a RIS with N reflective elements, and K single-antenna users, green elements in RIS are passive, yellow elements in RIS are active: (a) Cascade channel estimation, and (b) separate channel estimation.

Stacking T time slots of Equation (1) and combining Equation (2), by assuming $x_{k,t} = 1$ the received signal $\boldsymbol{Y}_k = [\boldsymbol{y}_{k,1}, \boldsymbol{y}_{k,2}, \cdots, \boldsymbol{y}_{k,T}] \in \mathbb{C}^{M \times T}$ can be expressed as:

$$\boldsymbol{Y}_k = \boldsymbol{G}\boldsymbol{\phi} + \boldsymbol{N}_k \tag{3}$$

where $\boldsymbol{\phi} = [\phi_1, \phi_2, \cdots, \phi_T] \in \mathbb{C}^{N \times T}$ and $N_k = [n_{k,1}, n_{k,2}, \cdots, n_{k,T}] \in \mathbb{C}^{M \times T}$. With the finite scattering properties of mmWave, it can be represented using the Saleh-Valenzuela (SV) model [21–24]. The channel matrix $\boldsymbol{H}$ between the RIS and the BS can be written as:

$$\boldsymbol{H} = \sum_{l=1}^{L} \alpha_l \boldsymbol{a}_N(\psi_l, v_l) \boldsymbol{a}_M^{\mathrm{H}}(\omega_l, \mu_l) \tag{4}$$

where L represents the propagation scattering path between the BS and the RIS; α_l, (ψ_l, v_l) and (ω_l, μ_l) are the complex gain, angle of arrival (AoA) and angle of departure (AoD) of the lth path, respectively. The channel matrix $\boldsymbol{h}_k$ between user k and the RIS can be written as:

$$\boldsymbol{h}_k = \sum_{j=1}^{J_k} \beta_{k,j} \boldsymbol{a}_N(\varphi_{k,j}, \theta_{k,j}), \quad \forall k \in K \tag{5}$$

where J_k represents the propagation scattering path between the k users and the RIS; $\beta_{k,j}$ and $(\varphi_{k,j}, \theta_{k,j})$ are the complex gain and AOD of the jth path to the kth user, respectively. A steering vector of the $P = P_1 \times P_2$ UPA is $\boldsymbol{a}_P(z, x) \in \mathbb{C}^{P \times 1}$, which can be expressed as [21–23]:

$$\boldsymbol{a}_P(z, x) = \boldsymbol{a}_{P_1}(z) \otimes \boldsymbol{a}_{P_2}(x) \tag{6}$$

where $\boldsymbol{a}_{P_1}(z)$ and $\boldsymbol{a}_{P_2}(z)$ can be expressed as (7) and (8), respectively:

$$\boldsymbol{a}_{P_1}(z) = [1, \mathrm{e}^{-\mathrm{j}2\pi z}, \cdots, \mathrm{e}^{-\mathrm{j}2\pi(P_1-1)z}] \tag{7}$$

$$\boldsymbol{a}_{P_2}(x) = [1, \mathrm{e}^{-\mathrm{j}2\pi x}, \cdots, \mathrm{e}^{-\mathrm{j}2\pi(P_2-1)x}] \tag{8}$$

where the variables z and x can be considered as the corresponding equivalent spatial frequencies with respect to the z axis and x axis of the UPA, respectively. The $\boldsymbol{a}_{P_1}(z)$ and $\boldsymbol{a}_{P_2}(x)$ are the two uniform linear array (ULA) on the vertical (z-axis) and horizontal (x-axis) directions, respectively. The UPA is obtained by performing a Kronecker product calculation from two ULA. The $\rho \in [-90°, 90°]$ and $\xi \in [-180°, 180°]$ are expressed as the signal elevation and azimuth angles of the UPA, respectively. The relationship between the spatial frequency pair (z, x) and the physical angle pair (ρ, ξ) exists as [22]:

$$z = \frac{d}{\lambda} \cos(\rho), \quad x = \frac{d}{\lambda} \sin(\rho) \cos(\xi) \tag{9}$$

where λ is the carrier wavelength, d is the component spacing. We assume a one-to-one correspondence between physical angle and spatial frequency on the UPA side, then it is necessary to satisfy $d \leq \lambda/2$.

The following evaluation metrics are commonly used in RIS channel estimation. Mean squared error (MSE) and normalised MSE (NMSE) are used to express the accuracy of channel estimation commonly. The MSE and NMSE can be expressed as (10) and (11), respectively:

$$e_{\mathrm{MSE}} = \mathbb{E}\left[\left\|\hat{\boldsymbol{G}} - \boldsymbol{G}\right\|_{\mathrm{F}}^2\right] \tag{10}$$

$$e_{\mathrm{NMSE}} = \mathbb{E}\left[\frac{\left\|\hat{\boldsymbol{G}} - \boldsymbol{G}\right\|_{\mathrm{F}}^2}{\left\|\boldsymbol{G}\right\|_{\mathrm{F}}^2}\right] \tag{11}$$

where $\hat{G}$ is the estimated value. The signal-to-noise ratio (SNR) represents the ratio of signal power to noise power. The SNR can be expressed as:

$$r_{\text{SNR}} = \frac{P_{\text{S}}}{P_{\text{N}}} \tag{12}$$

where P_{S} is the signal power and P_{N} is the power of the noise. The pilot overhead is also one of the important metrics for evaluating channel estimation methods. The bit error rate (BER) and achievable rate can indicate the efficiency of the message delivery after channel estimation and beamforming.

3.1. Channel Estimation for RIS Systems in High Frequency Bands

In this section, we focus on the channel estimation for RIS systems in high frequency bands. As one of the key technologies of 5G, the larger bandwidth of mmWave brings larger channel capacity and higher communication rates. Higher band THz is also considered one of the key technologies for future 6G development. However, the path propagation process generates severe path loss and the path is easily blocked by obstacles, the hardware complexity and huge power consumption associated with the high frequency bands are the main problems it currently faces. The RIS, with its low cost, low power consumption and the advantage of reducing the path loss by reflecting the signal, can make up for the shortage in the high frequency bands. Accurate CSI can design the optimal phase dependence of RIS and thus improve the performance, while the accuracy of channel estimation determines the acquisition of CSI. A suitable method with high accuracy, low training overhead and complexity is difficult to achieve at the same time slot when selecting a method for channel estimation.

In the high frequency bands, multipath scattering is sparse and can be modeled by the angular domain. This modeling approach uses only a small number of parameters, which reduces the pilot overhead. the RIS cannot transmit or receive signals due to its passive characteristic, therefore the channel estimation is accomplished by designing from the hardware and transmission protocol aspects. In terms of hardware design, there are fully-passive RIS and semi-passive RIS. The difference is that fully-passive RIS is passive reflective element that can only reflect signals, while semi-passive RIS can receive signals by installing a small number of active elements. Due to the difference in hardware, the existing channel estimation methods can be divided into cascaded channel estimation and individual channel estimation.

In the mmWave band, due to its channel sparsity, only the angle, gain and time delay need to be estimated for channel estimation, and the required pilot overhead is reduced greatly. In the RIS-assisted wireless communication system, cascaded channel estimation methods and separated channel estimation methods have their own advantages and disadvantages. The channel estimation methods in high frequency bands are described in Figure 3. Methods are based on fully passive RIS and semi-passive RIS in different scenarios, which are divided into four main aspects: single-user, multi-user, practical application, and wideband systems.
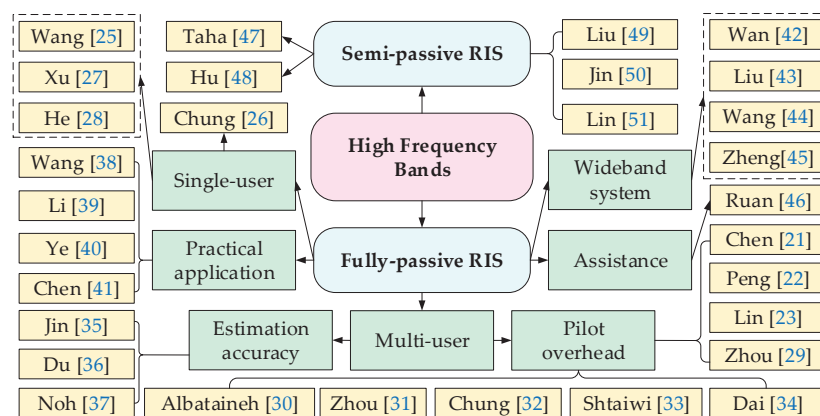

Figure 3. Channel estimation for RIS systems in high frequency bands.

3.1.1. Channel Estimation for Fully-Passive RIS

Single-user: With passive characteristics of fully-passive RIS, it cannot complete the reception and transmission of the signal. Therefore the existing channel estimation method is to complete the estimation of the cascaded channel, as shown in Figure 2(a). To achieve good reflection characteristics, the channels of BS-RIS and RIS-UE are considered as the overall channel, and the CSI obtained through the cascaded channel is sufficient to complete the phase shift setting of the RIS. The sparsity of mmWave can be exploited to convert the channel estimation problem into a sparse channel recovery problem, which can be solved using a compressive sensing (CS) algorithm.

Wang et al. [25] converted the channel estimation problem into a sparse recovery representation of the cascaded channel using the property of Khatri-Rao and Kronecker products. The problem was solved using the orthogonal matching pursuit (OMP) and generalized approximate message passing (GAMP) algorithm. In channel estimation, excessive training overhead can lead to a reduction in signal efficiency. Therefore different approaches are proposed in the following.

Chung et al. [26] proposed two-stage beam training and channel estimation method based on fast alternating least square (FALS), which can reduce the complexity. The training overhead can to be reduced by recovering the complete channel matrix using the observed partial channel matrix.

Deep learning methods have attracted much attention in recent years and can be effectively applied to channel estimation. Xu et al. [27] proposed a channel subsampling and a two-part deep neural network (DNN) approach to reduce the training overhead in dynamic time-varying channels. The first part describes the RIS dynamic channel using the neural ordinary differential equation (ODE), and the latter part uses the ODE to modify the structure of the neural network to complete the channel extrapolation. He et al. [28] simulated a conventional gradient descent algorithm using a model-driven depth unfolding approach. A computationally intensive training process was performed in the offline phase, and only low-complexity computations are required in the projection phase. The method has the advantage of low pilot overhead.

Multi-user: More pilot overhead and interference among UEs are needed to be considered in multi-user scenarios, therefore a more suitable method for estimation needs to be found.

Since the number of paths in the BS-RIS-UE will be little, unlike conventional MIMO mmWave channels where only row sparsity is available, in RIS-assisted mmWave communication systems with row block sparsity, this feature can be exploited to further reduce the training overhead [24]. To reduce training overhead and pilot overhead, Chen et al. [21] used row-column block sparsity on the foundation of [24]. Using this property, a method was proposed to exploit inter-user correlation to achieve joint channel recovery for multiple users. The proposed method reduces the pilot overhead compared to least square (LS), multiple measurement vector (MMV), etc.

Channel estimation efficiency can be improved by setting up a reasonable transmission protocol. To reduce the pilot overhead, the sparsity and correlation of mmWave multi-user was exploited in [22] and [29]. Partial information of single user can be estimated in the first. Further, the channel between BS and RIS is estimated in large time scale using the quasi-static property between BS-RIS, and the channel estimation of multi-user is completed using channel recovery. Also using the case that the physical locations of BS, RIS and UEs do not vary significantly over multiple consecutive channel coherence blocks, the remaining channel coherence blocks only need to estimate the rapidly varying channel gain.

Moreover, a RIS-assisted mmWave channel estimation method based on the Re'nyi entropy function was proposed in [30]. The Re'nyi entropy function is utilized as a sparse promoting regularizer for the purpose of reducing the pilot overhead. When utilizing CS algorithms, the complexity is cube proportional to the number of RIS components. Lin et al. [23] transform the channel estimation problem into a fixed constraint rank one parametric regularization optimization problem. The manifold optimisation (MO) and alternating minimisation (AM) methods are used to find the local optimal solution. To further reduce the complexity, a three-part CS-based channel estimation method was proposed [23].

To improve the estimation performance and robustness, in sparse channel recovery, a predefined dictionary is used, which leads to grid mismatch and performance degradation. Zhou et al. [31] proposed to optimize the dictionary to adapt to the channel characteristics. BS and RIS keep the position constant in most cases. Chung et al. [32] estimated the angular information by using the position information. The atomic norm minimization (ANM) based channel estimation method is further proposed to achieve the purpose of reducing the pilot overhead.

To improve the ability to apply different scenarios and reduce the pilot overhead, Shtaiwi et al. [33] first estimate some of the active users and in the second stage estimate inactive users based on the spatial-temporal-spectral (STS) framework of deep convolutional neural networks (CNN). Deep learning networks can sometimes have a low generalisation ability and cannot be applied to changing scenarios. Take it a step further, Dai et al. [34] proposed distributed machine learning (DML) technique to achieve reliable downlink cascaded channel estimation and neural network architectures.

Deep learning is an effective way to improve the estimation performance. Three practical residual neural networks, namely, generative adversarial networks based convolutional blind denoising (GAN-CBD) network, convolutional blind denoising network (CBDNet) and multiple residual dense network (MRDNet), were proposed in [35] using the low-rank structure of the channel. Specifically, the GAN-CBD and CBDNet based on the generative adversarial network were used in the offline phase to obtain accurate CSI, and then the MRDNet was used to adapt the online cascaded channel estimation with improved generalization and fitting capabilities flexibly. A semi-blind joint channel estimation and symbol detection scheme was proposed in [36]. The method proves that the BS received signal follows the PARATUCK2 tensor model and there is no training phase, and symbol detection and channel estimation are done simultaneously. It is difficult to meet the demand for a large number of training symbols in practice, and two Cramér-Rao lower bound (CRB)-based training signal design methods for enhanced sparse channel estimation were proposed in [37]. The CRB for the channel parameters consisting of path gain and path angle is derived under the assumption of Bayesian mixture parameters.

Practical application: The impact of its hardware cost and accidents on RIS needs to be considered. The increase in the number of antennas in large scale MIMO systems leads to high power consumption and high cost, Wang et al. [38] proposed to equip the BS with a small number of analog-to-digital converters (ADC). The channel estimation is then completed using the bilinear generalized approximate message passing (BiG AMP) algorithm.

To address the information loss due to quantization, a Bayesian optimal estimation framework was introduced to reduce the cost and power consumption. RIS was proposed in [39] to apply low precision ADC quantization in large scale MIMO communication systems. Further, a channel estimation algorithm based on GAMP algorithm and combined with expectation maximization (EM) and nearest neighbor learning (NNL) algorithms was proposed. It compensate for the loss caused by low precision ADC quantization, which can guarantee the estimation performance while reducing power consumption.

To solve array blocking problems caused by sand, dust, rain and snow cover in practical applications. The joint array diagnosis and channel estimation methods applied to single-user and multi-user were proposed in [39], respectively. It reduced the influence caused by the outside world and improved the channel estimation accuracy and usage efficiency.

To eliminate inter-cell and intra-cell interference, Ye et al. [40] achieved a proper phase shift for each element design by designing different reflection coefficients. It ensures that the performance of the desired user is maximised and that interference to the undesired user is minimised. An efficient two-dimensional line spectrum optimization based on ANM was also proposed for channel estimation, and the designed of reflection beam formation was accomplished using this method, but the method was limited when the number of users increases.

Integrating RIS into vehicles achieves good applications in the future. The mobility of vehicles makes the CSI change constantly, which makes it difficult to obtain accurate instantaneous CSI.

Therefore a transmission protocol with a reasonable configuration of CSI acquisition time scale was proposed in [41], which can reduce the channel information update frequency, and the proposed method can reduce the complexity and training overhead effectively.

Wideband systems: The proposed method for narrowband systems is not well applicable in wideband systems generally. Wan et al. [42] proposed to use OFDM to overcome frequency selective fading in wideband, and then use BS-RIS a prior knowledge to design the pilot to estimate BS-UE and RIS-UE by the distributed OMP (DOMP) method jointly. Liu et al. [43] transformed the wideband channel estimation into a parameter recovery problem. Several pilot symbols were used to detect the channel parameters by a newtonian OMP (NOMP) algorithm. This method considered the phase and delay differences between the received signals at different BS antennas and RIS elements.

Wang et al. [44] applied the super-resolution (SR) method in images to channel estimation. Then they proposed a switch-based method for LS estimation and super-resolution, which can reduce the training overhead while ensuring the channel estimation accuracy.

Zheng et al. [45] proposed a channel estimation method based on canonical polyadic decomposition (CPD) by representing the received signal as a third-order tensor using the inherent sparsity of mmWave. Then the channel parameters are estimated based on the structured CPD method.

The problem of high pilot overhead due to a fully-passive RIS can often also be solved by assisted methods. Ruan et al. [46] proposed an approach of using reference points for separate channel estimation to overcome the problem of large training overhead for cascaded channels.

Due to the passive characteristic of the RIS, setting up active elements in the passive RIS to estimate the channels of the BS-RIS and RIS-UE separately. In the next part of this section, the fully-passive hardware architecture of the RIS changes to a semi-passive structure, and the corresponding channel estimation methods change.

3.1.2. Channel Estimation for Semi-Passive RIS

The fully-passive RIS can perform cascaded channel estimation due to the inability to transmit and receive signals mostly. Due to the inability to decouple well in high-dimensional channels and the scaling ambiguity, it is difficult to obtain CSI for BS-RIS and RIS-UE. Therefore several active RIS elements are proposed to be placed in the RIS, as shown in Figure 2(b), which can both exploit the advantages of RIS in saving power to a certain extent and accomplish signal processing more efficiently.

An architecture with only a few active elements was proposed in [47]. A CS method was proposed to perform channel reconstruction for sampled channels sensed by a few elements. Another method was to use deep learning to learn the best mapping from the best reflection matrix.

Hu et al. [48] proposed a receiver element RIS structure equipped with only a portion of 1-bit quantization. The training signal at the passive RIS element was first recovered using the alternating direction method of multipliers (ADMM), and then the full channel information was obtained using channel sparsity and the GAMP algorithm.

A deep denoising neural network-assisted compressed channel estimation method was proposed in [49]. The complete channel matrix was obtained from partial cells using the channel reconstruction method, and the estimation accuracy was further improved using denoising neural networks.

Jin et al. [50] proposed an approach to reshape the channel matrix into a two-dimensional image, using single-scale enhanced deep super-resolution (EDSR) neural network and multi-scale deep super-resolution (MDSR) neural network to recover the channel using low sparse channel properties. The approach can increase the generalization capability and reduce the hardware complexity.

Lin et al. [51] considered time-varying channels, proposed a hybrid RIS structure composed of active and passive elements. the narrowband was modeled as a third-order CPD problem and the wideband problem as a fourth-order CPD problem. Then the tensor problem was solved by an algebraic method to recover the channel parameters and complete the channel estimation. This can help to improve the accuracy of estimating and reduce the complexity of estimating.

The channel estimation algorithms and performance comparison in high frequency bands are described in Table 2. Table 2 describes the methods from four aspects: system setup, problem, method, and results analysis.

Table 2. Channel estimates in high frequency bands sorted by publication years.

Ref.	Year	System Setup	Problem	Method	Results Analysis
Wang et al. [25]	2020	MISO	High training overhead	Conversion to sparse channel recovery problem	Approximate NMSE of 0.04 obtained using the GAMP algorithm
Wan et al. [42]	2020	MIMO	Wideband system estimation issues	DOMP algorithm and redundant dictionary	Pilot design and redundant dictionaries can improve performance significantly
Liu et al. [49]	2020	MIMO	High training overhead	The deep denoising neural network assisted compressive channel estimation	4 dB performance gain over initial estimation
Chung et al. [32]	2021	MIMO	High training overhead	Location-aware channel estimation based on ANM	2D ANM location awareness was only at 32 training symbols, 3D ANM maximum training symbols was 32, both better than 1D ANM
Shtaiwi et al. [33]	2021	MIMO	High training overhead	Estimate active users and use CNN's STS framework to estimate inactive users	The larger the number of active users, the smaller the NMSE
Li. [39]	2021	MIMO	High cost/array block	An EM-NNL-GAMP method/Joint array diagnosis and channel estimation algorithm	Outperformed other algorithms at 2 bit/Different methods for different situations were effective for array diagnosis and channel estimation
Liu et al. [43]	2021	MIMO	High pilot overhead	Convert a parameter recovery problem and use NOMP algorithm	Low SNR and small number of pilots had better performance than OMP
Wang et al. [44]	2021	SISO	High training overhead	SR method in images	10% rate improvement compared to LS (SNR = 35 dB)
Taha et al. [47]	2021	MIMO	High training overhead	Reconstruction of the full channel from subsampled channels using CS and deep learning	Achieved 90% of the best rates
Hu et al. [48]	2021	MIMO	High hardware cost and energy consumption	The semi-passive RIS equipped with a partial 1-bit quantization, ADMM and GAMP algorithms	Better than baseline at high SNR
Jin et al. [50]	2021	MIMO	Low estimation accuracy	Reshape the channel matrix into a two-dimensional image	As the proportion of active cells increases, EDSR had better NMSE performance and MDSR reduced complexity

Continued

Ref.	Year	System Setup	Problem	Method	Results Analysis
Lin et al. [51]	2021	MIMO	The problem of time-varying channels	Modeling as a CPD problem and solving tensor problems with algebraic algorithm	Reduced complexity and great results at high SNR
Chung et al. [26]	2022	MISO	High training overhead	Two-stage beam training and FALS	FALS required 45% fewer training symbols compared to the OMP and ANM algorithms (NMSE = 0.1)
Xu et al. [27]	2022	MISO	High training overhead	Deep DNN assisted compressed channel estimation algorithm	NMSE decreased with increasing spatial and temporal sampling
Zhou et al. [29]	2022	MISO	High training overhead	Multi-user correlation, channel sparsity, invariance of channel coherence blocks	60% reduction in pilot overhead compared to baseline scheme (NMSE $= 10^{-3}$)
Peng et al. [22]	2022	MIMO	High training overhead	A three-stage estimation protocol using the correlation between typical users and normal users	50% reduction in pilot overhead compared to OMP (NMSE $= 10^{-2}$)
Albataineh et al. [30]	2022	MIMO	High Pilot overhead	Extends the Re'nyi entropy function as the sparsity-promoting regularizer	An improvement over the OMP
Lin et al. [23]	2022	MIMO	Inefficient method	A MO and AM based method and a three-stage algorithm	The MO method had good results when the overhead was higher than 130. The CS method proposed in this paper is better than GAMP
Zhou et al. [31]	2022	MISO	Grid mismatch issues and estimation performance degradation	Dictionary is optimized to adapt to channel characteristics	Better than the predefined dictionary method when the training overhead was small
He et al. [28]	2022	SIMO	High training overhead	The model-driven deep unfolding neural network	Achieved the same NMSE with 25% less training overhead than LS
Dai et al. [34]	2022	MIMO	High training overhead	The DML algorithm	Used in different scenarios
Jin et al. [35]	2022	MIMO	Low estimation accuracy	GAN-CBD, CBDNet and MRDNet	MRDNet achieved better NMSE performance than GAN-CBD and CBDNet, with improvements of 5.63 dB and 4.51 dB, respectively
Du et al. [36]	2022	MIMO	Low estimation accuracy	Semi-blind joint channel estimation and symbol detection algorithm	Better NMSE and BER performance
Noh et al. [37]	2022	MIMO	Less training symbols	Two CRB-based training signal design algorithms for enhanced sparse channel estimation	Significant performance gain when the number of training symbols was less than the number of RIS reflection elements

Continued

Ref.	Year	System Setup	Problem	Method	Results Analysis
Ye et al. [40]	2022	SISO	Interference problems	Maximize power at desired users and eliminate interference at undesired users	The reflector element changed from 8 to 16, achieved a power gain of approximately 10 dB
Chen et al. [41]	2022	MIMO	High mobility leads to CSI changes and requires high overhead	A reasonable configuration of the CSI acquisition time scale	The communication performance was improved in mobile vehicle scenarios
Zheng et al. [45]	2022	MIMO	High training overhead	The received signal is represented as a low-rank third-order tensor	Significantly reduced training overhead and better performance compared to SOMP algorithm
Ruan et al. [46]	2022	MIMO	High training overhead	Used reference points to aid estimation	NMSE was reduced by 2 dB compared to the best benchmark solution (SNR = 10 dB)
Chen et al. [21]	2023	MIMO	High training overhead	Two-stage channel estimation method using common sparse structure	80% and 60% pilot overhead reduction in LS and MMV respectively (NMSE = 10^{-2})
Wang et al. [38]	2023	MIMO	High cost	Low-resolution ADCs and Bayesian optimal estimation framework	The BiG AMP algorithm had better performance in few bit quantization, and 8 bit quantization was almost as good as infinite bit quantization

3.2. Channel Estimation for RIS Systems in Low Frequency Bands

In this section, the focus is on the channel estimation method for RIS systems in low frequency bands. At low frequency bands due to its rich multipath scattering, an unstructured channel model is used, but the method is difficult to describe the overall characteristics of the propagation environment. Unstructured CSI requires a large training overhead, therefore many channel estimation methods have been proposed to reduce the training overhead.

The channel estimation methods in low frequency bands are described in Figure 4. Methods are based on fully-passive RIS and semi-passive RIS in different scenarios, which are divided into four main aspects: MISO, MIMO, massive MIMO, and wideband system.
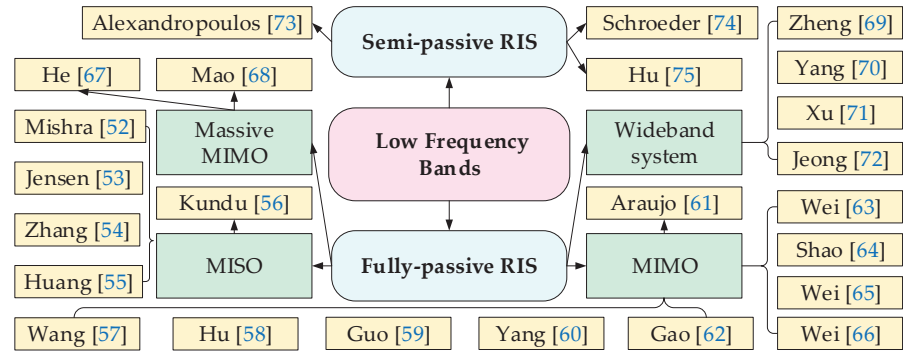

Figure 4. Channel estimation for RIS systems in low frequency bands.

The channel estimation methods of different RIS systems are presented by different RIS architectures. Similar to the high band, the fully-passive RIS mostly uses the estimation method of cascaded channels, while the semi-passive can use the method of separate channel estimation.

3.2.1. Channel Estimation for Fully-Passive RIS

In a fully-passive RIS assisted low frequency system, channel estimation can be accomplished for the cascaded channel. And the obtained CSI is sufficient to accomplish setting the optimal phase to achieve maximum transmission efficiency. The methods applied will be varied for different system settings, and we will present the channel estimation methods for different system settings in the following.

MISO systems: Mishra et al. [52] first proposed the ON/OFF channel estimation method. The method accomplishes channel estimation by sequentially turning on the RIS element. Since the cascaded channels are only estimated one by one, the estimated variance of each element is equal to 2. To reduce the variance, A minimum variance unbiased (MVU) estimator was proposed in [53]. This method get good estimation accuracy, while it required large pilot overhead.

To further reduce the pilot overhead, different approaches were proposed in [54,55]. Zhang et al. [54] proposed a rank-one matrix factorization (MF) approach. AM and gradient descent methods were then used to find the approximate optimal solution. An iterative expectation maximization (EM) algorithm for semi-blind channel estimation was proposed in [55]. The method first transforms the channel estimation problem into a maximum likelihood estimation problem. By initializing the semi-blind channel estimation with a pilot and solving it using EM.

Kundu et al. [56] proposed an linear minimum mean square error (LMMSE) based channel estimation method that further utilized CNN to approximate the optimal solution. Both denoising CNN (DnCNN) and fast and flexible denoising network (FFDNet) are considered in this paper. Improved MSE performance of DnCNN and FFDNet-based channel estimators as channels become more highly correlated. This method offered high performance and relatively low implementation complexity.

MIMO systems: The increased number of users and antennas can make channel estimation more challenging. In [57], a three-stage channel estimation method was proposed considering the redundancy among channels without any assumption of sparsity and low rank. The channel matrix of a typical user directly to the BS and the channel matrix reflected by the RIS were estimated in the first two stages, respectively. Finally the channel estimation of other users was completed using the strong correlation between other users and that user. This can reduce the pilot overhead and save estimation time in MIMO systems.

Hu et al. [58] used the quasi static property of BS-RIS to perform channel estimation at the time scale. Small-scale channel estimation was performed between UE and RIS, which can reduce the pilot overhead significantly. This property is used in later channel estimation methods frequently.

A normally open training protocol was proposed in [59] and utilized a common link structure to reduce the pilot overhead. An optimization-based channel estimation problem was further proposed using the covariance of cascaded channels. The alternating optimization algorithm was then used in order to find the locally optimal solution.

To reduce the training overhead, Yang et al. [60] proposed the anchor-assisted approach, which assisted RIS in channel estimation by setting anchor points. The tensor modeling approach is also applicable to channel estimation.

Dearaujo et al. [61] proposed channel estimation method relying on parallel factor (PARAFAC) of received signal tensor modeling. This method dealt with the non-ideal case, when there is phase perturbation and when the receiver does not know the RIS phase shift.

Deep learning methods have received much attention in recent years and can be applied to channel estimation to achieve better performance. Gao et al. [62] proposed a three-stage DNN framework, which can achieve better performance without relying on high pilot overhead and accurate channel statistics.

A cascaded channel estimation scheme based on dual-structured orthogonal matching tracking (DS-OMP) was proposed in [63] by exploiting dual structural sparsity of inter-user angular cascade channels.

In RIS assisted wireless communication systems, not all devices are active at the same time, and assigning potential devices to pilot sequences as well would lead a excessive overhead. Shao et al. [64] proposed a unsourced random access (URA) scheme and proposed a rank one decomposition-based message recovery and channel estimation method for RIS-assisted URAs. Both channel estimation and signal recovery alone require a lot of training and computation, therefore [65] and [66] proposed joint channel estimation and signal recovery methods that were able to cost lower complexity.

Massive MIMO systems: The larger number of antennas can make channel estimation more difficult to achieve. To complete the channel estimation, He et al. [67] proposed a two-stage cascaded channel estimation method. In the first stage, a BiG AMP algorithm with sparse matrix decomposition was used. In the second stage, a matrix-completed Riemannian streamlined gradient algorithm was used to accomplish accurate channel estimation. The size of sparsity affects matrix decomposition and completion.

The deep learning approach is further utilized. Mao et al. [68] brought the results of channel recovery into the residual network, to reduce the errors caused by grid mismatch. In order to improve the accuracy of the OMP algorithm, a residual structure-based OMP (RS-OMP) network was proposed. Then a straightforward network (SN) structure was proposed instead of the OMP algorithm.

Wideband systems: Zheng et al. [69] designed a novel phase-shifted channel estimation model for RIS-OFDM systems that satisfies the unit-mode constraint. Yang et al. [70] proposed a method using RIS grouping in SISO systems. Both methods provide accurate channel estimation results and a reduction in training overhead.

Xu et al. [71] extrapolated the partial RIS elements to the complete channel by closing them and obtaining partial channel information. Using the compression idea, the extrapolation problem was transformed into a problem of recovering the channel parameters. The complete channel was reconstructed using the sparse Bayesian learning (SBL) framework finally. This method can reduce the pilot overhead while ensuring the accuracy.

In OFDM systems, the carrier frequency offset problem is encountered. Jeong et al. [72] proposed a joint carrier frequency offset (CFO) and channel impulse response (CIR) estimation method to solve this problem. The method improved the channel estimation accuracy under OFDM systems.

3.2.2. Channel Estimation for Semi-Passive RIS

The estimation of separate channels can be easily accomplished by setting active elements with transceiver signal capability installed on the RIS. However, in semi-passive RIS, it is necessary to consider not only the method of channel estimation, but also to set the number and location of active RIS elements in a reasonable way. The goal is to be able to improve the accuracy or reduce the complexity of channel estimation while ensuring that the hardware complexity and power consumption are acceptable.

An architecture consisting of a passive RIS and an active RF chain for baseband reception was proposed in [73]. Using this architecture and assuming sparse wireless channels in the beamspace domain, an alternating optimization method was proposed to achieve explicit channel estimation on the RIS side. This method save pilot overhead and training time.

Schroeder et al. [74] proposed a two-stage channel estimation scheme based on ANM. A new two-stage channel estimation approach was developed in a hybrid RIS architecture. The proposed channel estimation required less number of active RIS elements and only one-way training, which has better estimation performance.

Hu et al. [75] proposed a semi-passive RIS using a grouping structure. Based on this structure, a two-stage channel estimation method was proposed. The first stage estimated the BS-RIS channel signal parameters by the estimation of signal parameters via rotational invariance technique (ESPRIT). The second stage estimated the channel using the total least squares (TLS) ESPRIT and multi-signal classification (MUSIC) methods. This method has better performance and lower training overhead, and the performance can be further improved by flexibly allocating the training time between the two

phases. Best performance is achieved when the ratio of first stage to total time is 0.1. But grouping structure made the beamforming performance degraded.

The channel estimation algorithms and performance comparison in low frequency bands are described in Table 3. Table 3 describes the methods from four aspects: system setup, problem, method, and results analysis.

Table 3. Channel estimates in low frequency bands sorted by publication years.

Ref.	Year	System Setup	Problem	Method	Results Analysis
Mishra et al. [52]	2019	MISO	Fully-passive RIS cannot handle signals	ON/OFF method	Binary channel estimation method
Jensen et al. [53]	2020	MISO	RIS increases the number of estimated links	MVU	Estimation accuracy was T (training periods) times better than the ON/OFF method
Wang et al. [57]	2020	MIMO	High training overhead	The relevance of typical user and other users	Improve estimation performance, more time slots should be allocated for the second stage to reduce error propagation
He et al. [67]	2020	MIMO	RIS can't send and receive signals	Sparse matrix decomposition stage and matrix completion	Better than comparable matrix decomposition and matrix completion schemes.
Zheng et al. [69]	2020	SISO	High training overhead	Transmission protocol with sequential channel estimation and reflection optimization	14 dB gain improvement over ON/OFF method at the same pilot overhead
Yang et al. [70]	2020	SISO	High training overhead	Elements grouping	Better achievable rates than methods without RIS component grouping
Alexandropoulos et al. [73]	2020	SISO	High training overhead	RIS architecture with a single RF	Produced best estimation performance with smaller training symbols than OMP and LS algorithms
Zhang et al. [54]	2021	MISO	High training overhead	Matrix factorization	Lower overhead and higher accuracy
Kun et al. [56]	2021	MISO	Low estimation accuracy	FFDNET and DNCNN	FFDNET outperformed DNCNN at low SNR but required noise variance information
Hu et al. [58]	2021	MIMO	High training overhead	BS-RIS quasi-static features	Reduced pilot overhead, but worse performance than MVU
Dearaujo et al. [61]	2021	MIMO	High training overhead	PARAFAC tensor modeling of the received signal	Robustness for amplitude and phase perturbations
Gao et al. [62]	2021	MIMO	High training overhead	Integrated DNN to estimate the direct channel, active RIS and inactive RIS sequentially	50% reduction in pilot overhead compared to OMP (NMSE = 10^{-2})
Wei et al. [63]	2021	MIMO	High training overhead	Cascaded channel estimation scheme based on DS-OMP	Improved NMSE performance as the number of common paths increased

Continued

Ref.	Year	System setup	Problem	Method	Results Analysis
Wei et al. [65]	2021	MIMO	Large complexity for both channel estimation and signal recovery	Joint channel estimation and signal recovery algorithm	Only about 2.5 dB performance difference compared to LS scheme assuming perfect channel knowledge
Huang et al. [55]	2022	MISO	High cost/array block	Iterative EM algorithm for semi-blind channel estimation	85% reduction in pilot overhead compared to baseline scheme (NMSE = 10^{-2})
Guo et al. [59]	2022	MIMO	High training overhead	Alternating optimization algorithms and cascaded channel covariance	Approximately 15 dB performance gain over ON/OFF method
Yang et al. [60]	2022	MIMO	High training overhead	Anchor-assisted channel estimation	Approximately 50 training symbols can be reduced for the same performance as the baseline scheme
Shan et al. [64]	2022	MIMO	High training overhead	A rank one decomposition-based message recovery and channel estimation algorithm for RIS-assisted URAs	Better separation than baseline solution for active devices
Wei et al. [66]	2022	MIMO	Large complexity for both channel estimation and signal recovery	Joint channel estimation and signal recovery method	Approximately 18 dB gap from baseline approach when pilot length = 100
Mao et al. [68]	2022	MIMO	Grid mismatch issues and performance degradation	Residual networks to reduce NMSE	SN worked well at small training overheads, RS-OMP achieved better results at large training overheads
Xu et al. [71]	2022	MIMO	High training overhead	Subsampled information is extrapolated to the full channel	12 dB performance gain compared to LS (The number of active RIS elements was 1/16 of the total RIS elements)
Jeong et al. [72]	2022	SISO	Carrier frequency offset	A joint CFO and CIR estimation	Up to 30 times higher performance relative to benchmark solutions
Schroeder et al. [74]	2022	MIMO	Low estimated efficiency	Two-stage channel estimation scheme based on ANM	Better performance than passive RIS
Hu et al. [75]	2022	MIMO	High training overhead	ESPRIT, TLS, MUSIC	Better performance than OMP and LMMSE methods

4. Signal Processing Algorithms for RIS Channel Estimation

Based on different parameter acquisition schemes and mathematical modeling, we divide channel estimation algorithms into four aspects: conventional-based, CS-based, deep learning-based, and composition-based algorithms.

4.1. The Conventional Algorithms for RIS Channel Estimation

In the generic channel estimation method, the transmitter transmits the pilot sequence and the receiver receives the signal sequence to recover the channel matrix in the constructed channel model.

LS/LMMSE: LS estimation [76] and LMMSE is a classical method for finding model solutions for channel estimation, which was used in RIS-aided systems for pilot-based channel estimation widely. The RIS channel estimation of conventional LS/LMMSE has a large channel estimation pilot overhead, to minimize the LS/LMMSE channel estimation error, the training reflection pattern and the transmit pilot sequence can be designed jointly [77,78].

The conventional LS estimation scheme had a high pilot overhead, which was reduced in [79]. Using a low-rank subspace, a reduced subspace LS estimation scheme and the RIS phase shift pattern was optimized to minimize the MSE of the channel estimation. Xu et al. [80] applied minimum MSE (MMSE) channel estimation to unmanned aerial vehicle (UAV) scenarios with low-complexity optimization of the RIS phase shift matrix.

At high Doppler frequencies, the existing RIS channel estimation techniques assuming block fading model pairs cause large errors. In [81], the characteristic of Doppler frequency shift of the time-varying channel leads to a large estimation overhead. To reduce the computational complexity, a correlation coefficient between direct line-of-sight and non-line-of-sight was established. The function of the channel was modeled and the MMSE estimation process was refined to improve the accuracy.

Grouping RIS: To reduce the training overhead and make full use of the spatial correlation of the channel, a scheme of grouping RIS elements was proposed in [70]. The large RIS was divided into several small RIS groups and each group shared the same common reflection coefficients, which was widely used in the subsequent RIS channel estimation process.

For the channel estimation problem of the uplink channel of a RIS-assisted multi-user MIMO (MU-MIMO) system, the entire RIS surface was divided into sub-RISs and an algorithm for estimating the channel using the symmetric positive definite (SPD) matrix [82] was proposed.

Kalman filtering (KF): The channel coefficient matrix was kept constant during the coherent time and the channel was estimated for the elements of the multiple time blocks [83]. Mao et al. [84] used KF for mobile scenes and derived the best reflection coefficients for RIS elements according to the MMSE .

For downlink communication system in a frequency division duplex MIMO system, Cai et al. [85] proposed that the direct channel and the cascaded channel were estimated by two KF tracking. The reflection coefficients at the pilot and RIS were designed jointly and the optimal coefficient matrix was approximated by the columns of the discrete Fourier transform (DFT) matrix.

Multi-stages: To further improve the estimation accuracy, the distributed multi-stage algorithm was used for RIS channel estimation widely. To obtain higher accuracy channel estimation with lower pilot overhead, in [86], an anchor-assisted multi-stage multiuser wideband cascaded channel estimation scheme was proposed to estimate the cascaded channels. In the first stage, Qian et al. [86] obtained BS-RIS CSI based on cyclic prefix single carrier transmission and phase configuration at RIS. In the second stage, the cascade channel information was estimated in the frequency domain using partial BS-RIS channel states.

Optimisation: The generalized EM (GEM) algorithm is used to estimate the parameters in the absence of variables, and the model and parameters are adjusted to obtain the optimal solution continuously. A spatially alternating GEM-based scheme for RIS-assisted channel measurements was presented in [87]. The scheme was estimated by multipath component tracking and maximum likelihood (ML) calculations.

In [88], a new over-the-air (OTA) method to estimate the true phase shift of the RIS elements was modeled as a high-dimensional non-convex optimization problem. The ML estimates were obtained by iterative algorithm. The root MSE (RMSE) of the phase estimation was closed to the CRB, thus verifying the effectiveness of the proposed algorithm.

The conventional-based channel estimation algorithms and performance comparison are described in Table 4. Table 4 describes the methods from four aspects: antenna/RIS architecture, channel model, major algorithm, and performance analysis.

Table 4. Comparison of conventional algorithms for RIS channel estimation.

Ref.	Year	Antenna/RIS Architecture	Channel Model	Major Algorithm	Performance Analysis
Zhou et al. [76]	2021	MIMO/Passive RIS	Static channel	AoA estimation and LS method	Improved estimation accuracy
Demir et al. [79]	2022	Passive RIS	Static channel	Reduced-subspace LS and array geometry	Reduced pliot overhead
Xu et al. [80]	2022	Passive RIS	Time-Varying and double selective Channel	MMSE and the end-to-end system model	Reduced computational complexity
Shtaiwi et al. [82]	2021	MIMO/Passive RIS	Static channel	SPD and Maximum-margin matrix factorization	Improved the estimation accuracy
You et al. [83]	2020	MIMO/Passive RIS	Time-varying channel	RIS-elements grouping and partition	Reduced computational complexity
Mao et al. [84]	2021	MIMO/Passive RIS	Time-varying channel	MMSE, KF and state-space model	Improved the estimation accuracy
Cai et al. [85]	2021	MIMO/Passive RIS	Time-varying channel	KF and codebook-based low complexity design	Reduced computational complexity and improved estimation accuracy
Xu et al. [81]	2023	Passive RIS	High-dimensional and high-Doppler reflected fading channels	MMSE interpolation and multiplicative concatenation of the channel coefficient	Improved estimation accuracy
Qian et al. [86]	2023	MIMO/Passive RIS	Static channel	Two-phase and anchor-aided channel estimation	Reduced polit overhead and improved estimation accuracy
Xu et al. [87]	2022	MIMO/Passive RIS	Static channel	Space-alternating GEM and ML estimation	Improved estimation accuracy
Zhang et al. [88]	2023	Passive RIS	Static channel	ML and CRB	Improved estimation accuracy

4.2. Compressed Sensing-Based Algorithms for RIS Channel Estimation

The problem is formulated as an optimization algorithm to recover the original signal as accurately as possible from the sparse projection matrix, which is often used to deal with the channel estimation problem of RIS [89].

The greedy algorithm, a common algorithm for CS, has low computational complexity and is often used in the signal recovery process [90,91]. Common CS techniques such as ANM [74], OMP algorithm [63], approximation messaging passing (AMP) [92], tensor decomposition technique [36] were widely used for channel estimation process. The CS algorithm constantly searches for the most suitable transform base to represent the channel matrix as sparse, which is an optimization problem. The channel matrix is computed accurately using a small amount of information, which reduces the pilot overhead during channel estimation significantly.

OMP algorithm: The conventional OMP algorithm directly used for RIS channel estimation leads to large complexity, and how to reduce the training overhead becomes a topic worth discussing. The number of RIS components is large and the calculated pressure of the composite channel is high. For

the composite channel models, the channel estimation problem was formulated as a sparse recovery problem for a set of independent dictionaries in the angular and temporal domains.

The computational complexity of the multidimensional OMP strategy was [93] based on compressed channel estimation, which was greatly reduced by not computing on the large dictionary directly. The OMP algorithm was modified to exploit the joint corner-domain sparse structure of the cascaded channels associated with different users. The matrices of the corner domain channels for different users had common non-zero rows. The joint estimation of a large number of common corner domain cascaded channels increased the number of training samples and reduced the effect of noise.

AMP algorithm: The sparsity of the OMP algorithm is a fixed value, which is not compatible with the actual situation. The further proposed AMP algorithm has adaptive sparsity. A two-stage algorithm including matrix decomposition stage and matrix completion stage was proposed in [67]. The RIS-assisted communication in the special scenario had a low distance between the RIS and the communication device, the channel coefficient matrix was a low-rank channel matrix.

In [92], in the first stage, conventional channel training methods were used to estimate the direct MIMO channel among UE terminals. In the second stage, the bilinear adaptive vector approximation messaging algorithm was used for dictionary matrix learning. The sparsity of the phase-shifted coefficient matrix was used to remove the permutation ambiguity from the channel during the training process. By using the statistical properties of the user-to-RIS and RIS-to-BS channels and the central limit theorem (CLT), It can verify the approximate Gaussian distribution when the channel propagates in the sub-6 GHz band.

By using Gaussian approximation, the joint channel estimation and data detection technique of the BiG AMP algorithm [94] was proposed. In the improved BiG AMP algorithm, a pilot was used to eliminate the effect of quantization and the paper used a quantization-aware approach to estimate the CSI. The performance was further improved relative to Ref. [92].

During numerical processing, the row sparse matrix elements were coupled to each other causing a certain degree of error in the conventional estimation scheme. A hybrid approximate message passing framework was proposed in [95] to decompose the derivative frequency matrix, and recover the row sparse representation in the model. The hybrid architecture compensates for the problem that GAMP cannot operate in the non-Gaussian distribution dictionary.

In this section we give an overview of the idea and use of CS algorithms in the RIS channel estimation process, mainly describing the shortcomings of the classical OMP algorithm, such as high computational complexity and fixed sparsity leading to large application limitations. The extension literature improves on the shortcomings, how to reduce the computational complexity, and the joint adaptive sparsity AMP algorithm.

The compressed sensing-based channel estimation algorithms and performance comparison are described in Table 5. Table 5 describes the methods from four aspects: antenna/RIS architecture, channel model, major algorithm, and performance analysis.

Table 5. Comparison of compressed sensing-based algorithms for RIS channel estimation.

Ref.	Year	Antenna/RIS Architecture	Channel Model	Major Algorithm	Performance Analysis
He et al. [67]	2020	MIMO/Passive RIS	Time-varying channels	Sparse matrix factorization and completion	Improved channel estimation accuracy
Mirza et al. [92]	2021	MIMO/Passive RIS	Static channel	Bilinear generalized AMP	Balanced the quality of channel estimation with training overhead

					Continued
Ref.	Year	Antenna/RIS Architecture	Channel model	Major algorithm	Performance analysis
Bayraktar et al. [93]	2022	Passive RIS	Static channel	Multidimensional OMP	Reduced computational complexity and improved estimation accuracy
Xiong et al. [94]	2023	MIMO/Passive RIS	Static channel	Bilinear generalized AMP	Reduced computational complexity
Zhou et al. [95]	2022	MIMO/Passive RIS	Static channel	Generalized-AMP	Reduced computational complexity and training overhead
Wu et al. [96]	2022	MIMO/Passive RIS	Static channel	Three-step OMP	Reduced pilot overhead

4.3. Deep Learning-Based Algorithms for RIS Channel Estimation

Deep learning has been used for RIS channel estimation [97,98] widely. The learning ability of neural networks can be used to estimate the full channel from the partial pilot channel information [99, 100], it can also be combined with image processing techniques to imagine the RIS channel information as two images. One corresponding to the real part channel information and one corresponding to the imaginary part channel information. Image processing techniques are more mature, and common interpolation and denoising methods for images are further applied in RIS. The coarse channel information is extracted, preprocessed and then trained in the network to get the accurate CSI image. The introduction of image processing techniques has opened up a new area worth exploring for CSI [101,102].

Most of the data processed by the channel estimation are complex numbers, but the existing deep learning library functions do not support the operation of the complex number domain. The general practice is that the data need to be preprocessed before input to the network, and the real and imaginary parts of the complex numbers are extracted, and then input to the neural network. Due to two kinds of real numbers without mining the phase information of the complex numbers, this preprocessing scheme brings much information loss.

The deep learning-based algorithms for RIS channel estimation are presented by different network architectures, which are divided into six main aspects: end to end, CNN, graph attention network (GANet), DNN, recurrent neural network (RNN), long short-term memory (LSTM).

End to end network: Existing RIS systems have separate functions for coding and modulation, channel estimation, channel equalisation, decoding, and demodulation. Actually, these modules can be also considered as a whole and modelled as an end to end network. The end to end network can further optimise the performance of the system by avoiding the system falling into local optima. Simultaneously optimized the connection weight coefficients of the sender, RIS and receiver to minimize the cross-entropy loss function of the system [99].

CNN network: Ahmet et al. [103] designed CNN networks for direct channel and cascade channel estimation, where the users accessed the network directly to estimate their own channels. A large amount of reflective surface channel informations were coupled with each other, which were computationally difficult. Compensated learning-based neural network was proposed in [104] to dynamically track the CSI. Due to the powerful adaptive capability of deep learning networks, the estimation process learned the fading channel knowledge directly without a priori knowledge. Chen et al. [104] reduced the number of hidden nodes and introduced an offset learning module to improve the performance in the network.

In practical scenarios, with large amount of data high-dimensional channels, the optimal MMSE estimates were difficult to obtain. Kundu et al. [56] proposed a deep learning-based data-driven

scheme to further approximate the MMSE estimation results. This method modelled the channel estimation as an image problem, using CNN networks to denoise and approximate the optimal MMSE channel results.

Liu et al. [105] developed a deep residual learning (DReL) framework applied to multi-user cascaded RIS channel estimation. The correctness of DReL is verified by applying it to CNN networks using Bayesian estimation theory derivation, avoiding the multi-dimensional integral calculation of MMSE estimation. The accuracy of channel estimation is further improved by exploiting the advantages of CNN and DReL in feature extraction and denoising.

GANet: Tekbiyik et al. [106] used GANet for full duplex wireless communication link channel estimation. The training results are robust under different propagation channels with better performance compared to conventional LS estimation.

DNN: During the estimation of partially activated RIS element channel coefficients, a three-stage estimation scheme was proposed in [62] for direct channel. Active RIS element cascade channel and inactive RIS element cascade channel was continuously trained to achieve good accuracy. Jin et al. [35] used residual neural networks for cascaded channel estimation. The offline trained neural network was based on convolutional blind denoising and convolutional blind denoising networks of generative adversarial networks. The online cascade channel estimation was proposed to use the network as a multi-residual dense network.

As shown in Figure 5, Zhang et al. [107] proposed a deep learning network architecture for RIS channel estimation.
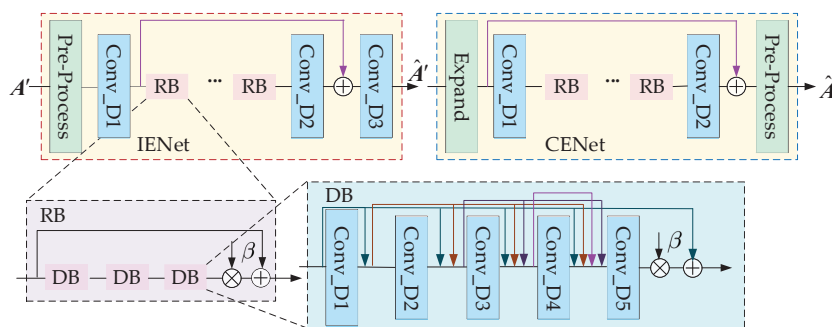

Figure 5. A deep learning network architecture for RIS channel estimation.

To reduce the pilot overhead, a strategy of RIS grouping was used. The grouping assumes that each group of RIS shares the same reflection coefficient, which is not consistent with reality and causes channel interference under a certain degree. Zhang et al. [107] designed two deep learning networks. The first network eliminates channel interference when RIS grouping was used, and the second network extrapolated the full channel from a partial channel. To separate the A' real part from the imaginary part, the network consists of 3 convolutional layers and multiple residual blocks (RB) of the same structure. Each RB contains 3 identical dense blocks (DB), each DB consists of 5 convolutional layers. A leaky rectified linear unit (LReLU) was used as the activation function for the first 4 layers in a DB. The output feature information from the previous layers was used as input to each subsequent convolutional layer, and $\hat{A}'$ was the output of IENet to improved estimation accuracy for the partial channels. the result learned by the nonlinear transformations, was multiplied by a constant β and then added to the result. CENet was constructed from 2 convolutional layers and the same RBs. $\hat{A}$ was the output of CENet. In turn, all channel information was obtained.

RNN: Considering the large number of RIS components and the relatively short coherence time, Xu et al. [27] considered a deep learning scheme to infer the full channel from partial channels in the antenna domain. Xu et al. used a RNN network in the time domain to explore the connection among different time blocks. The neural ODE to modify the relationship among different network data layers, modifying the network structure and improving the estimation performance of the time series, which is better suited for time-varying channel estimation scenarios.

In [108], the deep deterministic policy gradient based scheme was developed to adapt to the dynamic channel variations to suppress the interference of time-varying channels. Machine learning for channel estimation using reinforcement learning correlation algorithms was not applicable in RIS systems. For the RIS phase shift problem, the data samples associated with the transition from one state to another, it was difficult to define. In [109], a deep neural network model consisting of two DNN was proposed, that was more effective for a large number of RIS elements.

LSTM: In [110] exploited the dual time-scale channel property, where the BS and RIS channels were static and the channel between the RIS and the user was dynamic. In the subsequent channel estimation process, Xu et al. designed a LSTM based neural network framework for the channel decomposition process and the channel prediction process. Xu et al. changed the connection layer according to the nonlinear mapping relationship between the input and the output thus reducing the complexity.

The specific application scenarios of various network architectures in the process of RIS channel estimation were described above. Suitable networks improve channel estimation performances in unfavorable scenarios such as high-speed time-varying, noisy, etc.

The deep learning-based channel estimation algorithms and performance comparison are described in Table 6. Table 6 describes the methods from four aspects: antenna/RIS architecture, channel model, major algorithm, and performance analysis.

Table 6. Deep learning-based algorithms comparison for RIS channel estimation.

Ref.	Year	Antenna/RIS Architecture	Channel Model	Major Algorithm	Performance Analysis
Xu et al. [27]	2022	Passive RIS	Time-varying Channel	Ordinary differential equation, recurrent neural network	Improved estimation accuracy and robustness
Jin et al. [35]	2022	Passive RIS	Static channel	GAN-CBD, CBDNet and MRDNet	Got better generalisation and fitting ability
Kundu et al. [56]	2021	Passive RIS	Static channel	Denoising CNN	Reduced computational complexity and improved estimation accuracy
Gao et al. [62]	2021	MIMO/ Semi-passive RIS	Static channel	Three-stage training strategy for RNN	Reduced pilot overhead and improved estimation accuracy
Ahmetm et al. [103]	2020	Passive RIS	Static channel	CNN	Improved channel estimation accuracy
Chen et al. [104]	2022	MIMO/Passive RIS	Static channel	Learning-based CNN	Reduced computational complexity and improved channel estimation accuracy
Tekbiyik et al. [106]	2021	Passive RIS	Static channel	Graph attention network	Enhanced system robustness and reduced pilot overhead
Liu et al. [105]	2022	MIMO/Passive RIS	Static channel	Deep residual network and CNN	Improved estimation accuracy
Zhang et al. [107]	2021	Passive RIS	Static channel	Deep learning, channel extrapolation	Improved estimation accuracy and enhanced network generalisation
Xu et al. [108]	2020	Passive RIS	Time-varying channels	Deep reinforcement learning	Increased system capacity and suppressed interference
Li et al. [109]	2023	MIMO/Passive RIS	Static channel	Double deep learning	Reduced computational complexity

Continued

Ref.	Year	Antenna/RIS Architecture	Channel Model	Major Algorithm	Performance Analysis
Xu et al. [110]	2022	Passive RIS	Time-varying channel	Sparse-connected LSTM	Improved estimation accuracy, reduced time delay and pilot overhead

4.4. Composition-based Algorithms for RIS Channel Estimation

The direction of algorithm evolution has been described and it is found that deep learning algorithms are being intergrated with conventional algorithms and used in the channel estimation process widely. Deep learning can make up for the shortcomings of conventional algorithms, such as improving the channel estimation accuracy and joint optimization of multiple modules. The deficiencies of conventional algorithms with insufficient accuracy can be further improved by using the good denoising function of neural networks to improve the channel estimation accuracy.

SemiDefinite relaxation (SDR)-deep learning: Since elements on the RIS were usually arranged in two dimensions, treating the channel information as a single image. Yin et al. [111] first used a SDR scheme and then built an end to end deep learning channel prediction model that predicted the entire CSI based on the pilot information. It outperforms existing approaches based on grouping of RIS elements in terms of achievable rate.

LS-deep learning: Wang et al. [44] modelled the channel information estimated by LS as a low-resolution image and then interpolate it into a high-resolution image linearly.

OMP-deep learning: Using the conventional CS OMP algorithm, it is assumed that the arrival and departure angle bases fall on the discrete grid during the computation exactly, which does not match the reality causing errors. Mao et al. [68] fused deep learning in the OMP algorithm to get results after the residual network to improve the performance.

AMP-deep learning: Conventional CS algorithms AMP algorithm can reduce the pilot overhead substantially, but the estimation accuracy is insufficient. Tsai et al. [112] proposed a hypernetwork-assisted based learned AMP network with dynamic shrinkage parameters, where the adaptive shrinkage parameters of the network output are used among layers instead of a fixed value, thus improving the estimation accuracy.

The core of the conventional approach is in the human perception and modeling of the target problem, as well as proposing a solver to solve the model. Deep learning methods that use parameters to fit the problem can outperform conventional methods in case of good convergence. In most cases, the ability to fit a large number of network parameters is stronger than the models constructed using some prior knowledge in conventional methods. As the complexity of the problem increases, the advantage of deep learning becomes more obvious, the conventional solution incorporating deep learning solution has a broad development prospect.

The composition-based channel estimation algorithms and performance comparison are described in Table 7. Table 7 describes the methods from four aspects: antenna/RIS architecture, major algorithm, major algorithm, and performance analysis.

Table 7. Composition-based algorithms comparison for RIS channel estimation.

Ref.	Year	Antenna/RIS Architecture	Major Problem	Major Algorithm	Performance Analysis
Wang et al. [44]	2021	Passive RIS	High complexity of conventional algorithms	Proposed a high resolution network with low-precision by linear interpolation	Accuracy rate: 92% (SNR = 35 dB)

Continued

Ref.	Year	Antenna/RIS Architecture	Major problem	Major algorithm	Performance Analysis
Mao et al. [68]	2022	Passive RIS	Insufficient estimation performance of the CS algorithm	Proposed residual network to improve the performance	Outperformed the OMP (SNR = 35 dB)
Tsai et al. [112]	2022	MIMO/Passive RIS	Insufficient performance of AMP algorithm estimation	Proposed a hypernetwork-assisted LAMP network with dynamic shrinkage parameters	Reduced memory overhead: 50% and execution time: 93%
Yin et al. [111]	2022	Passive RIS	Insufficient performance of conventional algorithm estimation	Designed an end to end deep learning model	Reduced channel estimation overhead

5. Conclusions

RIS, as a fundamental and innovative technology, has great potential and development prospects in both 5G and future 6G. In this paper, we investigate the key of technology channel estimation for the emerging technology RIS. The focus is on investigating the channel estimation methods for RIS-assisted wireless communication systems in high and low frequency bands applications and the comparison under different channel estimation algorithms. Specifically, we first compare the RIS channel estimation methods in different frequency bands, and analyze the differences and development directions of channel estimation methods in fully-passive RIS and semi-passive RIS. We introduce a system model using angular domain modeling to accomplish channel estimation, in which fewer parameters can save training overhead.

We analyze the channel estimation methods in real situations, wideband and different system settings. Completing channel estimation in the real case requires consideration of cost, fault detection, and mobility issues. Issues such as frequency selective fading need to be considered in wideband, and issues such as mutual interference and pilot pollution need to be considered in different system settings. Therefore, different channel estimation methods need to be used in different scenarios.

We classify the channel estimation methods of RIS into conventional-based algorithms, CS-based algorithms, deep learning-based algorithms, composition-based algorithms, and investigate the application of channel estimation in RIS with different algorithms. We analyze the advantages and disadvantages of different methods, use the advantages and improve the disadvantages of different channel methods, and continuously search for more efficient channel estimation methods. We focus on emerging applications of deep learning in the field of RIS channel estimation, such as fusing deep learning with conventional solutions, combining the field of deep learning image processing with channel estimation and building end to end networks.

Finally, RIS has great potential for development in the future, and it is crucial to obtain accurate CSI to guarantee the efficient functioning of RIS. With the increase of cascaded links in multi-RIS systems, the channel estimation complexity increases further and the channel estimation method of single RIS may no longer be applicable. How to integrate more efficiently with RIS in higher frequency bands, such as the THz band, is also an issue of concern. Deploying RIS in complex and changing environments, such as cities with tall buildings, moving vehicles or satellites, requires more appropriate channel estimation methods to guarantee effective communication. The idea of fusing deep learning algorithms with conventional schemes and using the powerful data fitting capability of deep learning to improve the performance of conventional algorithms has a broad development prospect. In summary, RIS has great potential and deserves further exploration and research. We hope that this review can provide sufficient information and promote the development of RIS, about which the method of RIS channel estimation is still an evolving process.

Institutional Review Board Statement: Not applicable.

Informed Consent Statement: Not applicable.

Data Availability Statement: Not applicable.

Conflicts of Interest: The author declare no conflict of interest.

References

1. Liu, Y.; Liu, X.; Mu, X.; Hou, T.; Xu, J.; Di Renzo, M.; Al-Dhahir, N. Reconfigurable intelligent surfaces: Principles and opportunities. *IEEE Commun. Surv. Tutor.* **2021**, *23*, 1546–1577. https://doi.org/10.1109/COMST.2021.3077737.

2. Dajer, M.; Ma, Z.; Piazzi, L.; Prasad, N.; Qi, X.F.; Sheen, B.; Yang, J.; Yue, G. Reconfigurable intelligent surface: Design the channel – A new opportunity for future wireless networks. *Digit. Commun. Netw.* **2022**, *8*, 87–104. https://doi.org/10.1016/j.dcan.2021.11.002.

3. Zhao, Y.; Lv, X. Network coexistence analysis of RIS-assisted wireless communications. *IEEE Access* **2022**, *10*, 63442–63454. https://doi.org/10.1109/ACCESS.2022.3183139.

4. Wu, Q.; Zhang, S.; Zheng, B.; You, C.; Zhang, R. Intelligent reflecting surface-aided wireless communications: A tutorial. *IEEE Trans. Commun.* **2021**, *69*, 3313–3351. https://doi.org/10.1109/TCOMM.2021.3051897.

5. Papazafeiropoulos, A.; Abdullah, Z.; Kourtessis, P.; Kisseleff, S.; Krikidis, I. Coverage probability of STAR-RIS-assisted massive MIMO systems with correlation and phase errors. *IEEE Wirel. Commun. Lett.* **2022**, *11*, 1738–1742. https://doi.org/10.1109/LWC.2022.3179653.

6. Noh, S.; Lee, J.; Lee, G.; Seo, K.; Sung, Y.; Yu, H. Channel estimation techniques for RIS-assisted communication: Millimeter-wave and sub-THz systems. *IEEE Veh. Technol. Mag.* **2022**, *17*, 64–73. https://doi.org/10.1109/MVT.2022.3158765.

7. Elzwawi, G.H.; Elzuwawi, H.H.; Tahseen, M.M.; Denidni, T.A. Frequency selective surface-based switched-beamforming antenna. *IEEE Access* **2018**, *6*, 48042–48050. https://doi.org/10.1109/ACCESS.2018.2850808.

8. Zhang, L.; Chen, X.Q.; Liu, S.; Zhang, Q.; Zhao, J.; Dai, J.Y.; Bai, G.D.; Wan, X.; Cheng, Q.; Castaldi, G.; et al. Space-time-coding digital metasurfaces. *Nat. Commun.* **2018**, *9*, 4334. https://doi.org/10.1038/s41467-018-06802-0.

9. Tan, X.; Sun, Z.; Jornet, J.M.; Pados, D. Increasing indoor spectrum sharing capacity using smart reflect-array. In Proceedings of the IEEE International Conference on Communications; IEEE: Kuala Lumpur, Malaysia, 2016; pp. 1–6. https://doi.org/10.1109/ICC.2016.7510962.

10. Li, Z.; Chen, W.; Cao, H. Beamforming design and power allocation for transmissive RMS-Based transmitter architectures. *IEEE Wirel. Commun. Lett.* **2022**, *11*, 53–57. https://doi.org/10.1109/LWC.2021.3120284.

11. Di Renzo, M.; Ntontin, K.; Song, J.; Danufane, F.H.; Qian, X.; Lazarakis, F.; de Rosny, J.; Phan-Huy, D.T.; Simeone, O.; Zhang, R.; et al. Reconfigurable intelligent surfaces vs. relaying: Differences, similarities, and performance comparison, 2020, [arXiv:cs, eess, math/1908.08747].

12. Pradhan, C.; Li, A.; Song, L.; Li, J.; Vucetic, B.; Li, Y. Reconfigurable intelligent surface (RIS)-enhanced two-way OFDM communications. *IEEE Trans. Veh. Technol.* **2020**, *69*, 16270–16275. https://doi.org/10.1109/TVT.2020.3038942.

13. Yang, Z.; Liu, Y.; Chen, Y.; Al-Dhahir, N. Machine learning for user partitioning and phase shifters design in RIS-aided NOMA networks. *IEEE Trans. Commun.* **2021**, *69*, 7414–7428. https://doi.org/10.1109/TCOMM.2021.3100866.

14. Zheng, B.; You, C.; Mei, W.; Zhang, R. A survey on channel estimation and practical passive beamforming design for intelligent reflecting surface aided wireless communications. *IEEE Commun. Surv. Tutor.* **2022**, *24*, 1035–1071. https://doi.org/10.1109/COMST.2022.3155305.

15. Pan, C.; Zhou, G.; Zhi, K.; Hong, S.; Wu, T.; Pan, Y.; Ren, H.; Renzo, M.D.; Swindlehurst, A.L.; Zhang, R.; et al. An overview of signal processing techniques for RIS/IRS-aided wireless systems. *IEEE J. Sel. Top. Signal Process.* **2022**, pp. 1–35. https://doi.org/10.1109/JSTSP.2022.3195671.

16. Jian, M.; Alexandropoulos, G.C.; Basar, E.; Huang, C.; Liu, R.; Liu, Y.; Yuen, C. Reconfigurable intelligent surfaces for wireless communications: Overview of hardware designs, channel models, and estimation techniques. *Intelligent and Converged Networks* **2022**, *3*, 1–32. https://doi.org/10.23919/ICN.2022.0005.

17. Liang, Y.C.; Chen, J.; Long, R.; He, Z.Q.; Lin, X.; Huang, C.; Liu, S.; Shen, X.S.; Di Renzo, M. Reconfigurable intelligent surfaces for smart wireless environments: Channel estimation, system design and applications in 6G networks. *Sci. China-Inf. Sci.* **2021**, *64*, 200301. https://doi.org/10.1007/s11432-020-3261-5.

18. Chen, Z.; Ma, X.; Han, C.; Wen, Q. Towards intelligent reflecting surface empowered 6G terahertz communications: A survey. *China Commun.* **2021**, *18*, 93–119. https://doi.org/10.23919/JCC.2021.05.007.

19. Basharat, S.; Khan, M.; Iqbal, M.; Hashmi, U.S.; Zaidi, S.A.R.; Robertson, I. Exploring reconfigurable intelligent surfaces for 6G: State-of-the-art and the road ahead. *IET Communications* **2022**, *16*, 1458–1474. https://doi.org/10.1049/cmu2.12364.

20. Babiker, J.M.S.D.; Huang, X. A survey channel estimation for intelligent reflecting surface (IRS). In *Cognitive Radio Oriented Wireless Networks and Wireless Internet*; 2022; Vol. 427, pp. 169–180. https://doi.org/10.1007/978-3-030-98002-3_12.

21. Chen, J.; Liang, Y.C.; Cheng, H.V.; Yu, W. Channel estimation for reconfigurable intelligent surface aided multi-user mmWave MIMO systems. *IEEE Trans. Wirel. Commun.* **2023**, pp. 1–17. https://doi.org/10.1109/TWC.2023.3246264.

22. Peng, Z.; Zhou, G.; Pan, C.; Ren, H.; Swindlehurst, A.L.; Popovski, P.; Wu, G. Channel estimation for RIS-aided multi-user mmWave systems with uniform planar arrays. *IEEE Trans. Commun.* **2022**, *70*, 8105–8122. https://doi.org/10.1109/TCOMM.2022.3214892.

23. Lin, T.; Yu, X.; Zhu, Y.; Schober, R. Channel estimation for IRS-assisted millimeter-wave MIMO systems: Sparsity-inspired approaches. *IEEE Trans. Commun.* **2022**, *70*, 4078–4092. https://doi.org/10.1109/TCOMM.2022.3168876.

24. Liu, H.; Yuan, X.; Zhang, Y.J.A. Matrix-calibration-based cascaded channel estimation for reconfigurable intelligent surface assisted multiuser MIMO. *IEEE J. Sel. Areas Commun.* **2020**, *38*, 2621–2636. https://doi.org/10.1109/JSAC.2020.3007057.

25. Wang, P.; Fang, J.; Duan, H.; Li, H. Compressed channel estimation for intelligent reflecting surface-assisted millimeter wave systems. *IEEE Signal Process. Lett.* **2020**, *27*, 905–909. https://doi.org/10.1109/LSP.2020.2998357.

26. Chung, H.; Kim, S. Efficient two-stage beam training and channel estimation for RIS-aided mwave systems via fast alternating least squares. In Proceedings of the IEEE International Conference on Acoustics, Speech and Signal Processing; IEEE: Singapore, Singapore, 2022; pp. 5188–5192. https://doi.org/10.1109/ICASSP43922.2022.9746094.

27. Xu, M.; Zhang, S.; Ma, J.; Dobre, O.A. Deep learning-based time-varying channel estimation for RIS assisted communication. *IEEE Commun. Lett.* **2022**, *26*, 94–98. https://doi.org/10.1109/LCOMM.2021.3127160.

28. He, J.; Wymeersch, H.; Di Renzo, M.; Juntti, M. Learning to estimate RIS-aided mmWave channels. *IEEE Wirel. Commun. Lett.* **2022**, *11*, 841–845. https://doi.org/10.1109/LWC.2022.3147250.

29. Zhou, G.; Pan, C.; Ren, H.; Popovski, P.; Swindlehurst, A.L. Channel estimation for RIS-aided multiuser millimeter-wave systems. *IEEE Trans. Signal Process.* **2022**, *70*, 1478–1492. https://doi.org/10.1109/TSP.2022.3158024.

30. Albataineh, Z.; Hayajneh, K.F.; Shakhatreh, H.; Athamneh, R.A.; Anan, M. Channel estimation for reconfigurable intelligent surface-assisted mmWave based on Re'nyi entropy function. *Sci Rep* **2022**, *12*, 22301. https://doi.org/10.1038/s41598-022-26672-3.

31. Zhou, Z.; Cai, B.; Chen, J.; Liang, Y.C. Dictionary learning-based channel estimation for RIS-aided MISO communications. *IEEE Wirel. Commun. Lett.* **2022**, *11*, 2125–2129. https://doi.org/10.1109/LWC.2022.3194585.

32. Chung, H.; Kim, S. Location-aware channel estimation for RIS-aided mmWave MIMO systems via atomic norm minimization, 2021, [arXiv:eess/2107.09222].

33. Shtaiwi, E.; Zhang, H.; Abdelhadi, A.; Han, Z. RIS-assisted mmWave channel estimation using convolutional neural networks. In Proceedings of the IEEE Wireless Communications and Networking Conference Workshops; IEEE: Nanjing, China, 2021; pp. 1–6. https://doi.org/10.1109/WCNCW49093.2021.9419974.

34. Dai, L.; Wei, X. Distributed machine learning based downlink channel estimation for RIS assisted wireless communications. *IEEE Trans. Commun.* **2022**, *70*, 4900–4909. https://doi.org/10.1109/TCOMM.2022.3175175.

35. Jin, Y.; Zhang, J.; Huang, C.; Yang, L.; Xiao, H.; Ai, B.; Wang, Z. Multiple residual dense networks for reconfigurable intelligent surfaces cascaded channel estimation. *IEEE Trans. Veh. Technol.* **2022**, *71*, 2134–2139. https://doi.org/10.1109/TVT.2021.3132305.

36. Du, J.; Luo, X.; Li, X.; Zhu, M.; Rabie, K.M.; Kara, F. Semi-blind joint channel estimation and symbol detection for RIS-empowered multiuser mmWave systems. *IEEE Commun. Lett.* **2023**, *27*, 362–366. https://doi.org/10.1109/LCOMM.2022.3212083.

37. Noh, S.; Yu, H.; Sung, Y. Training signal design for sparse channel estimation in intelligent reflecting surface-assisted millimeter-wave communication. *IEEE Trans. Wirel. Commun.* **2022**, *21*, 2399–2413. https://doi.org/10.1109/TWC.2021.3112173.

38. Wang, R.; Ren, H.; Pan, C.; Fang, J.; Dong, M.; Dobre, O.A. Channel estimation for RIS-aided mmWave massive MIMO system using few-bit ADCs. *IEEE Commun. Lett.* **2023**, *27*, 961–965. https://doi.org/10.1109/LCOMM.2023.3240499.

39. Li, B. Sparse channel estimation for reconfigurable intelligent surface assisted millimeter wave massive MIMO system. PhD thesis, University of Electronic Science and Technology of China, 2021.

40. Ye, J.; Kammoun, A.; Alouini, M.S. Reconfigurable intelligent surface enabled interference nulling and signal power maximization in mmWave bands. *IEEE Trans. Wirel. Commun.* **2022**, *21*, 9096–9113. https://doi.org/10.1109/TWC.2022.3172885.

41. Chen, Y.; Wang, Y.; Jiao, L. Robust transmission for reconfigurable intelligent surface aided millimeter wave vehicular communications with statistical CSI. *IEEE Trans. Wirel. Commun.* **2022**, *21*, 928–944. https://doi.org/10.1109/TWC.2021.3100492.

42. Wan, Z.; Gao, Z.; Alouini, M.S. Broadband channel estimation for intelligent reflecting surface aided mmWave massive MIMO systems. In Proceedings of the IEEE International Conference on Communications; IEEE: Dublin, Ireland, 2020; pp. 1–6. https://doi.org/10.1109/ICC40277.2020.9149146.

43. Liu, Y.; Zhang, S.; Gao, F.; Tang, J.; Dobre, O.A. Cascaded channel estimation for RIS assisted mmWave MIMO transmissions. *IEEE Wirel. Commun. Lett.* **2021**, *10*, 2065–2069. https://doi.org/10.1109/LWC.2021.3092147.

44. Wang, Y.; Lu, H.; Sun, H. Channel estimation in IRS-enhanced mmWave system with super-resolution network. *IEEE Commun. Lett.* **2021**, *25*, 2599–2603. https://doi.org/10.1109/LCOMM.2021.3079322.

45. Zheng, X.; Wang, P.; Fang, J.; Li, H. Compressed channel estimation for IRS-assisted millimeter wave OFDM systems: A low-rank tensor decomposition-based approach. *IEEE Wirel. Commun. Lett.* **2022**, *11*, 1258–1262. https://doi.org/10.1109/LWC.2022.3163661.

46. Ruan, C.; Zhang, Z.; Jiang, H.; Dang, J.; Wu, L.; Zhang, H. Approximate message passing for channel estimation in reconfigurable intelligent surface aided MIMO multiuser systems. *IEEE Trans. Commun.* **2022**, *70*, 5469–5481. https://doi.org/10.1109/TCOMM.2022.3182369.

47. Taha, A.; Alrabeiah, M.; Alkhateeb, A. Enabling large intelligent surfaces with compressive sensing and deep learning. *IEEE Access* **2021**, *9*, 44304–44321. https://doi.org/10.1109/ACCESS.2021.3064073.

48. Hu, J.; Yin, H.; Bjornson, E. MmWave MIMO communication with semi-passive RIS: A low-complexity channel estimation scheme. In Proceedings of the IEEE Global Communications Conference; IEEE: Madrid, Spain, 2021; pp. 1–6. https://doi.org/10.1109/GLOBECOM46510.2021.9685434.

49. Liu, S.; Gao, Z.; Zhang, J.; Renzo, M.D.; Alouini, M.S. Deep denoising neural network assisted compressive channel estimation for mmWave intelligent reflecting surfaces. *IEEE Trans. Veh. Technol.* **2020**, *69*, 9223–9228. https://doi.org/10.1109/TVT.2020.3005402.

50. Jin, Y.; Zhang, J.; Zhang, X.; Xiao, H.; Ai, B.; Ng, D.W.K. Channel estimation for semi-passive reconfigurable intelligent surfaces with enhanced deep residual networks. *IEEE Trans. Veh. Technol.* **2021**, *70*, 11083–11088. https://doi.org/10.1109/TVT.2021.3109937.

51. Lin, Y.; Jin, S.; Matthaiou, M.; You, X. Tensor-based algebraic channel estimation for hybrid IRS-assisted MIMO-OFDM. *IEEE Trans. Wirel. Commun.* **2021**, *20*, 3770–3784. https://doi.org/10.1109/TWC.2021.3053580.

52. Mishra, D.; Johansson, H. Channel estimation and low-complexity beamforming design for passive intelligent surface assisted MISO wireless energy transfer. In Proceedings of the IEEE International Conference on Acoustics, Speech and Signal Processing; IEEE: Brighton, United Kingdom, 2019; pp. 4659–4663. https://doi.org/10.1109/ICASSP.2019.8683663.

53. Jensen, T.L.; De Carvalho, E. An optimal channel estimation scheme for intelligent reflecting surfaces based on a minimum variance unbiased estimator. In Proceedings of the IEEE International Conference on Acoustics, Speech and Signal Processing; IEEE: Barcelona, Spain, 2020; pp. 5000–5004. https://doi.org/10.1109/ICASSP40776.2020.9053695.

54. Zhang, W.; Tay, W.P. Cost-efficient RIS-aided channel estimation via rank-one matrix factorization. *IEEE Wirel. Commun. Lett.* **2021**, *10*, 2562–2566. https://doi.org/10.1109/LWC.2021.3107547.

55. Huang, C.; Xu, J.; Zhang, W.; Xu, W.; Ng, D.W.K. Semi-blind channel estimation for RIS-assisted MISO systems using expectation maximization. *IEEE Trans. Veh. Technol.* **2022**, *71*, 10173–10178. https://doi.org/10.1109/TVT.2022.3182347.

56. Kundu, N.K.; McKay, M.R. Channel estimation for reconfigurable intelligent surface aided MISO communications: From LMMSE to deep learning solutions. *IEEE Open Journal of the Communications Society* **2021**, *2*, 471–487. https://doi.org/10.1109/OJCOMS.2021.3063171.

57. Wang, Z.; Liu, L.; Cui, S. Channel estimation for intelligent reflecting surface assisted multiuser communications: Framework, algorithms, and analysis. *IEEE Trans. Wirel. Commun.* **2020**, *19*, 6607–6620. https://doi.org/10.1109/TWC.2020.3004330.

58. Hu, C.; Dai, L.; Han, S.; Wang, X. Two-timescale channel estimation for reconfigurable intelligent surface aided wireless communications. *IEEE Trans. Commun.* **2021**, *69*, 7736–7747. https://doi.org/10.1109/TCOMM.2021.3072729.

59. Guo, H.; Lau, V.K.N. Uplink cascaded channel estimation for intelligent reflecting surface assisted multiuser MISO systems. *IEEE Trans. Signal Process.* **2022**, *70*, 3964–3977. https://doi.org/10.1109/TSP.2022.3193626.

60. Yang, W.; Li, M.; Liu, Q. A novel anchor-assisted channel estimation for RIS-aided multiuser communication systems. *IEEE Commun. Lett.* **2022**, *26*, 2740–2744. https://doi.org/10.1109/LCOMM.2022.3179298.

61. de Araujo, G.T.; de Almeida, A.L.F.; Boyer, R. Channel estimation for intelligent reflecting surface assisted MIMO systems: A tensor modeling approach. *IEEE J. Sel. Top. Signal Process.* **2021**, *15*, 789–802. https://doi.org/10.1109/JSTSP.2021.3061274.

62. Gao, S.; Dong, P.; Pan, Z.; Li, G.Y. Deep multi-stage CSI acquisition for reconfigurable intelligent surface aided MIMO systems. *IEEE Commun. Lett.* **2021**, *25*, 2024–2028. https://doi.org/10.1109/LCOMM.2021.3063464.

63. Wei, X.; Shen, D.; Dai, L. Channel estimation for RIS assisted wireless communications—Part II: An improved solution based on double-structured sparsity. *IEEE Commun. Lett.* **2021**, *25*, 1403–1407. https://doi.org/10.1109/LCOMM.2021.3052787.

64. Shao, X.; Cheng, L.; Chen, X.; Huang, C.; Ng, D.W.K. Reconfigurable intelligent surface-aided 6G massive access: Coupled tensor modeling and sparse Bayesian learning. *IEEE Trans. Wirel. Commun.* **2022**, *21*, 10145–10161. https://doi.org/10.1109/TWC.2022.3182653.

65. Wei, L.; Huang, C.; Alexandropoulos, G.C.; Yang, Z.; Yuen, C.; Zhang, Z. Joint channel estimation and signal recovery in RIS-assisted multi-user MISO communications. In Proceedings of the IEEE Wireless Communications and Networking Conference; IEEE: Nanjing, China, 2021; pp. 1–6. https://doi.org/10.1109/WCNC49053.2021.9417121.

66. Wei, L.; Huang, C.; Guo, Q.; Yang, Z.; Zhang, Z.; Alexandropoulos, G.C.; Debbah, M.; Yuen, C. Joint channel estimation and signal recovery for RIS-empowered multiuser communications. *IEEE Trans. Commun.* **2022**, *70*, 4640–4655. https://doi.org/10.1109/TCOMM.2022.3179771.

67. He, Z.Q.; Yuan, X. Cascaded channel estimation for large intelligent metasurface assisted massive MIMO. *IEEE Wirel. Commun. Lett.* **2020**, *9*, 210–214. https://doi.org/10.1109/LWC.2019.2948632.

68. Mao, Z.; Liu, X.; Peng, M. Channel estimation for intelligent reflecting surface assisted massive MIMO systems—A deep learning approach. *IEEE Commun. Lett.* **2022**, *26*, 798–802. https://doi.org/10.1109/LCOMM.2022.3147200.

69. Zheng, B.; Zhang, R. Intelligent reflecting surface-enhanced OFDM: Channel estimation and reflection optimization. *IEEE Wirel. Commun. Lett.* **2020**, *9*, 518–522. https://doi.org/10.1109/LWC.2019.2961357.

70. Yang, Y.; Zheng, B.; Zhang, S.; Zhang, R. Intelligent reflecting surface meets OFDM: Protocol design and rate maximization. *IEEE Trans. Commun.* **2020**, *68*, 4522–4535. https://doi.org/10.1109/TCOMM.2020.2981458.

71. Xu, X.; Zhang, S.; Gao, F.; Wang, J. Sparse Bayesian learning based channel extrapolation for RIS assisted MIMO-OFDM. *IEEE Trans. Commun.* **2022**, *70*, 5498–5513. https://doi.org/10.1109/TCOMM.2022.3184640.

72. Jeong, S.; Farhang, A.; Perovic, N.S.; Flanagan, M.F. Low-complexity joint CFO and channel estimation for RIS-aided OFDM systems. *IEEE Wirel. Commun. Lett.* **2022**, *11*, 203–207. https://doi.org/10.1109/LWC.2021.3124049.

73. Alexandropoulos, G.C.; Vlachos, E. A hardware architecture for reconfigurable intelligent surfaces with minimal active elements for explicit channel estimation. In Proceedings of the IEEE International Conference on Acoustics, Speech and Signal Processing; IEEE: Barcelona, Spain, 2020; pp. 9175–9179. https://doi.org/10.1109/ICASSP40776.2020.9053976.

74. Schroeder, R.; He, J.; Juntti, M. Channel estimation for hybrid RIS aided MIMO communications via atomic norm minimization. In Proceedings of the IEEE International Conference on Communications Workshops; IEEE: Seoul, Republic of Korea, 2022; pp. 1219–1224. https://doi.org/10.1109/ICCWorkshops53468.2022.9814534.

75. Hu, X.; Zhang, R.; Zhong, C. Semi-passive elements assisted channel estimation for intelligent reflecting surface-aided communications. *IEEE Trans. Wirel. Commun.* **2022**, *21*, 1132–1142. https://doi.org/10.1109/TWC.2021.3102446.

76. Zhou, G.; Pan, C.; Ren, H.; Wang, K. Channel estimation for RIS-aided millimeter-wave massive MIMO systems . In Proceedings of the 55th Asilomar Conference on Signals, Systems, and Computers; IEEE: Pacific Grove, CA, USA, 2021; pp. 698–703. https://doi.org/10.1109/IEEECONF53345.2021.9723140.

77. Zheng, B.; You, C.; Zhang, R. Intelligent reflecting surface assisted multi-user OFDMA: Channel estimation and training design. *IEEE Trans. Wirel. Commun.* **2020**, *19*, 8315–8329. https://doi.org/10.1109/TWC.2020.3021434.

78. Abeywickrama, S.; You, C.; Zhang, R.; Yuen, C. Channel estimation for intelligent reflecting surface assisted backscatter communication. *IEEE Wirel. Commun. Lett.* **2021**, *10*, 2519–2523. https://doi.org/10.1109/LWC.2021.3106165.

79. Demir, O.T.; Bjornson, E.; Sanguinetti, L. Exploiting array geometry for reduced-subspace channel estimation in RIS-aided communications. In Proceedings of the IEEE 12th Sensor Array and Multichannel Signal Processing Workshop; IEEE: Trondheim, Norway, 2022; pp. 455–459. https://doi.org/10.1109/SAM53842.2022.9827790.

80. Xu, C.; An, J.; Bai, T.; Xiang, L.; Sugiura, S.; Maunder, R.G.; Yang, L.L.; Hanzo, L. Reconfigurable intelligent surface assisted multi-carrier wireless systems for doubly selective high-mobility Ricean channels. *IEEE Trans. Veh. Technol.* **2022**, *71*, 4023–4041. https://doi.org/10.1109/TVT.2022.3147859.

81. Xu, C.; An, J.; Bai, T.; Sugiura, S.; Maunder, R.G.; Wang, Z.; Yang, L.L.; Hanzo, L. Channel estimation for reconfigurable intelligent surface assisted high-mobility wireless systems. *IEEE Trans. Veh. Technol.* **2023**, *72*, 718–734. https://doi.org/10.1109/TVT.2022.3203818.

82. Shtaiwi, E.; Zhang, H.; Vishwanath, S.; Youssef, M.; Abdelhadi, A.; Han, Z. Channel estimation approach for RIS assisted MIMO systems. *IEEE Trans. Cogn. Commun. Netw.* **2021**, *7*, 452–465. https://doi.org/10.1109/TCCN.2021.3075413.

83. You, C.; Zheng, B.; Zhang, R. Channel estimation and passive beamforming for intelligent reflecting surface: Discrete phase shift and progressive refinement. *IEEE J. Sel. Areas Commun.* **2020**, *38*, 2604–2620. https://doi.org/10.1109/JSAC.2020.3007056.

84. Mao, Z.; Peng, M.; Liu, X. Channel estimation for reconfigurable intelligent surface assisted wireless communication systems in mobility scenarios. *China Commun.* **2021**, *18*, 29–38. https://doi.org/10.23919/JCC.2021.03.003.

85. Cai, P.; Zong, J.; Luo, X.; Zhou, Y.; Chen, S.; Qian, H. Downlink channel tracking for intelligent reflecting surface-aided FDD MIMO systems. *IEEE Trans. Veh. Technol.* **2021**, *70*, 3341–3353. https://doi.org/10.1109/TVT.2021.3063138.

86. Qian, S.; Chen, Y.; Li, Q.; Li, P.; Xia, X.; Wen, M. Anchor-aided channel estimation for RIS-assisted multiuser broadband communications. *IEEE Wirel. Commun. Lett.* **2023**, *12*, 89–93. https://doi.org/10.1109/LWC.2022.3217827.

87. Xu, Y.; Wang, C.X.; Zhou, Z.; Feng, R.; Xin, L.; Huang, J. A novel SAGE-based channel parameter estimation scheme for 6G RIS-assisted wireless channel measurements. In Proceedings of the IEEE International Conference on Communications; IEEE: Seoul, Republic of Korea, 2022; pp. 3305–3310. https://doi.org/10.1109/ICC45855.2022.9839190.

88. Zhang, W.; Jiang, Y. Over-the-air phase calibration of reconfigurable intelligent surfaces. *IEEE Wirel. Commun. Lett.* **2023**, pp. 1–4. https://doi.org/10.1109/LWC.2023.3238479.

89. Ardah, K.; Gherekhloo, S.; de Almeida, A.L.F.; Haardt, M. TRICE: A channel estimation framework for RIS-aided millimeter-wave MIMO systems. *IEEE Signal Process. Lett.* **2021**, *28*, 513–517. https://doi.org/10.1109/LSP.2021.3059363.

90. Jia, C.; Cheng, J.; Gao, H.; Xu, W. High-resolution channel estimation for intelligent reflecting surface-assisted mmWave communications. In Proceedings of the IEEE 31st Annual International Symposium on Personal, Indoor and Mobile Radio Communications; IEEE: London, UK, 2020; pp. 1–6. https://doi.org/10.1109/PIMRC48278.2020.9217312.

91. Ma, X.; Chen, Z.; Chen, W.; Li, Z.; Chi, Y.; Han, C.; Li, S. Joint channel estimation and data rate maximization for intelligent reflecting surface assisted terahertz MIMO communication systems. *IEEE Access* **2020**, *8*, 99565–99581. https://doi.org/10.1109/ACCESS.2020.2994100.

92. Mirza, J.; Ali, B. Channel estimation method and phase shift design for reconfigurable intelligent surface assisted MIMO networks. *IEEE Trans. Cogn. Commun. Netw.* **2021**, *7*, 441–451. https://doi.org/10.1109/TCCN.2021.3072895.

93. Bayraktar, M.; Palacios, J.; Gonzalez-Prelcic, N.; Zhang, C.J. Multidimensional orthogonal matching pursuit-based RIS-aided joint localization and channel estimation at mmWave. In Proceedings of the IEEE 23rd International Workshop on Signal Processing Advances in Wireless Communication; IEEE: Oulu, Finland, 2022; pp. 1–5. https://doi.org/10.1109/SPAWC51304.2022.9833999.

94. Xiong, Y.; Qin, L.; Sun, S.; Liu, L.; Mao, S.; Zhang, Z.; Wei, N. Joint effective channel estimation and data detection for RIS-aided massive MIMO systems with low-resolution ADCs. *IEEE Commun. Lett.* **2023**, *27*, 721–725. https://doi.org/10.1109/LCOMM.2022.3232217.

95. Zhou, L.; Dai, J.; Xu, W.; Chang, C. Sparse channel estimation for intelligent reflecting surface assisted massive MIMO systems. *IEEE Trans. Green Commun. Netw.* **2022**, *6*, 208–220. https://doi.org/10.1109/TGCN.2022.3146188.

96. Wu, J.; Li, Y.; Xin, L. Joint channel estimation for RIS-assisted wireless communication system. In Proceedings of the IEEE Wireless Communications and Networking Conference; IEEE: Austin, TX, USA, 2022; pp. 1087–1092. https://doi.org/10.1109/WCNC51071.2022.9771916.

97. Huang, C.; Mo, R.; Yuen, C. Reconfigurable intelligent surface assisted multiuser MISO systems exploiting deep reinforcement learning. *IEEE J. Sel. Areas Commun.* **2020**, *38*, 1839–1850. https://doi.org/10.1109/JSAC.2020.3000835.

98. Yerzhanova, M.; Kim, Y.H. Channel estimation via model and learning for monostatic multiantenna backscatter communication. *IEEE Access* **2021**, *9*, 165341–165350. https://doi.org/10.1109/ACCESS.2021.3134961.

99. Jiang, H.; Dai, L.; Hao, M.; MacKenzie, R. End-to-end learning for RIS-aided communication systems. *IEEE Trans. Veh. Technol.* **2022**, *71*, 6778–6783. https://doi.org/10.1109/TVT.2022.3162624.

100. Zhang, Z.; Jiang, T.; Yu, W. Learning based user scheduling in reconfigurable intelligent surface assisted multiuser downlink. *IEEE J. Sel. Top. Signal Process.* **2022**, *16*, 1026–1039. https://doi.org/10.1109/JSTSP.2022.3178213.

101. Xu, J.; Ai, B. When mmWave high-speed railway networks meet reconfigurable intelligent surface: A deep reinforcement learning method. *IEEE Wirel. Commun. Lett.* **2022**, *11*, 533–537. https://doi.org/10.1109/LWC.2021.3135602.

102. Xu, M.; Zhang, S.; Zhong, C.; Ma, J.; Dobre, O.A. Ordinary differential equation-based CNN for channel extrapolation over RIS-assisted communication. *IEEE Commun. Lett.* **2021**, *25*, 1921–1925. https://doi.org/10.1109/LCOMM.2021.3064596.

103. Ahmet M., E.; Papazafeiropoulos, A.; Kourtessis, P.; Chatzinotas, S. Deep channel learning for large intelligent surfaces aided mm-wave massive MIMO systems. *IEEE Wirel. Commun. Lett.* **2020**, *9*, 1447–1451. https://doi.org/10.1109/LWC.2020.2993699.

104. Chen, Z.; Tang, J.; Zhang, X.Y.; Wu, Q.; Wang, Y.; So, D.K.C.; Jin, S.; Wong, K.K. Offset learning based channel estimation for intelligent reflecting surface-assisted indoor communication. *IEEE J. Sel. Top. Signal Process.* **2022**, *16*, 41–55. https://doi.org/10.1109/JSTSP.2021.3129350.

105. Liu, C.; Liu, X.; Ng, D.W.K.; Yuan, J. Deep residual learning for channel estimation in intelligent reflecting surface-assisted multi-user communications. *IEEE Trans. Wirel. Commun.* **2022**, *21*, 898–912. https://doi.org/10.1109/TWC.2021.3100148.

106. Tekbiyik, K.; Kurt, G.K.; Huang, C.; Ekti, A.R.; Yanikomeroglu, H. Channel estimation for full-duplex RIS-assisted HAPS backhauling with graph attention networks. In Proceedings of the IEEE International Conference on Communications; IEEE: Montreal, QC, Canada, 2021; pp. 1–6. https://doi.org/10.1109/ICC42927.2021.9500697.

107. Zhang, S.; Zhang, S.; Gao, F.; Ma, J.; Dobre, O.A. Deep learning-based RIS channel extrapolation with element-grouping. *IEEE Wirel. Commun. Lett.* **2021**, *10*, 2644–2648. https://doi.org/10.1109/LWC.2021.3110305.

108. Xu, J.; Ai, B.; Quek, T.Q.S.; Liuc, Y. Deep reinforcement learning for interference suppression in RIS-aided high-speed railway networks. In Proceedings of the IEEE International Conference on Communications Workshops; IEEE: Seoul, Republic of Korea, 2022; pp. 337–342. https://doi.org/10.1109/ICCWorkshops53468.2022.9814619.

109. Li, K.; Huang, C.; Gong, Y.; Chen, G. Double deep learning for joint phase-shift and beamforming based on cascaded channels in RIS-assisted MIMO networks. *IEEE Wirel. Commun. Lett.* **2023**, pp. 1–5. https://doi.org/10.1109/LWC.2023.3238073.

110. Xu, W.; An, J.; Xu, Y.; Huang, C.; Gan, L.; Yuen, C. Time-varying channel prediction for RIS-assisted MU-MISO networks via deep learning. *IEEE Trans. Cogn. Commun. Netw.* **2022**, *8*, 1802–1815. https://doi.org/10.1109/TCCN.2022.3188153.

111. Yin, S.; Li, Y.; Tian, Y.; Yu, F.R. Intelligent reflecting surface enhanced wireless communications with deep-learning-based channel prediction. *IEEE Trans. Veh. Technol.* **2022**, *71*, 1049–1053. https://doi.org/10.1109/TVT.2021.3129311.

112. Tsai, W.C.; Chen, C.W.; Teng, C.F.; Wu, A.Y. Low-complexity compressive channel estimation for IRS-aided mmWave systems with hypernetwork-assisted LAMP network. *IEEE Commun. Lett.* **2022**, *26*, 1883–1887. https://doi.org/10.1109/LCOMM.2022.3178188.